# FFT-Based Ridgelets For Radiative Transport

Bachelor Thesis by Simon Etter

Advisor: Axel Obermeier

Supervisor: Prof. Dr. Philipp Grohs

25 September 2013

ETH Zürich

# Contents


**1 Introduction** **3**
- 1.1 Radiative Transport Equation . . . 3
- 1.2 Ridgelets . . . 3

**2 Preliminaries** **5**
- 2.1 Discrete intervals . . . 5
- 2.2 Sobolev spaces . . . 5
- 2.3 Fourier Transform . . . 5
- 2.4 Finite Fourier Transform . . . 9

**3 Ridgelets** **14**
- 3.1 Construction . . . 14
- 3.2 Ridgelet Transform . . . 19
- 3.3 Finite Ridgelet Transform . . . 21

**4 Intermezzo: Scalar Products** **31**
- 4.1 Definitions . . . 31
- 4.2 Relations . . . 31

**5 Radiative Transport Equation** **34**
- 5.1 Basic RTE Solver . . . 34
- 5.2 Convergence Of Basic RTE Solver . . . 37
- 5.3 Discrete Ordinates Method . . . 40
- 5.4 Sparse Discrete Ordinates Method . . . 41
- 5.5 Source Iterations . . . 44

**6 Numerical Experiments** **45**
- 6.1 Convergence Of CG . . . 45
- 6.2 Convergence Of Basic RTE Solver . . . 49
- 6.3 General Dirichlet Boundary Conditions . . . 49
- 6.4 Convergence Of SDOM Compared To DOM . . . 55
- 6.5 Source Iterations . . . 55

**7 Conclusion** **62**

# 1 Introduction

## 1.1 Radiative Transport Equation

The radiative transport equation (RTE)

$$s \cdot \nabla u + \kappa\, u = f + \int_{\mathbb{S}^1} \sigma u \, ds'$$

is a steady state continuity equation describing the conservation of radiative intensity in an absorbing, emitting and scattering medium. Let us assume that the following quantities are known at all locations $(x, y) \in \Omega := [0, L_x) \times [0, L_y)$ and for all directions $s \in \mathbb{S}^1 := \{s \in \mathbb{R}^2 \mid \|s\|_2 = 1\}$:

- absorption coefficient $\kappa\,(x, y, s) \in \mathbb{R}$
- source term $f\,(x, y, s) \in \mathbb{R}$
- scattering kernel $\sigma\,(x, y, s, s') \in \mathbb{R}$

Then, the above equation allows us to find the unknown radiative intensity $u$ as a function $\Omega \times \mathbb{S}^1 \to \mathbb{R}$, which is the problem at the heart of this bachelor thesis.

Although the RTE looks simple, standard numerical techniques for solving it do not perform well for two reasons:

- The transport term $s \cdot \nabla u$ leads to ill-conditioned systems of equations.
- With the dimension of the domain of $u$ being 3 in 2-dimensional physical space and 5 in 3-dimensional space, the problem is fairly high-dimensional.

Both of these points make the accurate numerical solution of the RTE very costly or even impossible due to memory and compute power limitations of today's hardware. But there is hope that they can be mitigated by discretizing the RTE with a novel class of basis functions called ridgelets. This bachelor thesis investigates the benefits and drawbacks that come along with such an approach.

## 1.2 Ridgelets

At the most superficial level, a ridgelet is a function which "looks like a ridge", i.e. a function which is located along a line orthogonal to which it oscillates heavily and along which it varies only little (see Figure 1.1a for an example). Obviously, if we have several such ridgelets with varying locations, directions and widths, we can nicely represent

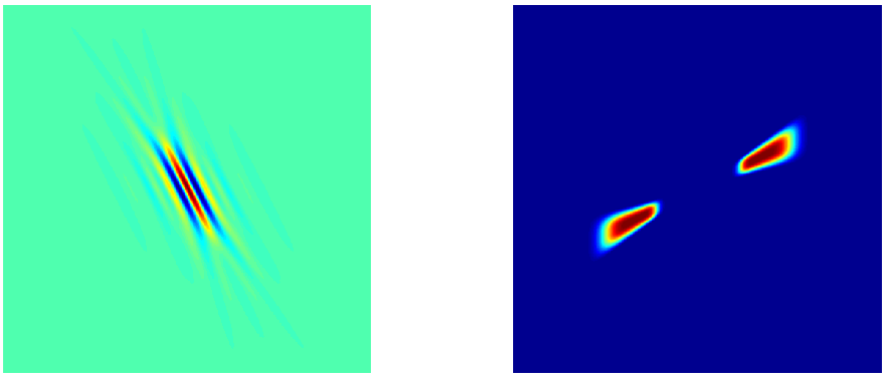

(a) An example ridgelet in real space (Green denotes 0)

(b) A similar ridgelet in Fourier space (Blue denotes 0)

Figure 1.1

a function whose features are located along curves by a linear combination of some (possibly few!) of them. Solutions of the RTE typically fall into this category of nicely representable functions as the variations along the transport direction are smoothed out while the ones orthogonal to it are not.

For the purpose of this bachelor thesis, this real space characterization of ridgelets is useful for getting an intuition on why ridgelets are well suited for a discretization of the RTE. If one wants to do some real work with these functions, however, a characterization in Fourier space comes in handier: In Fourier space, a ridgelet is located at some line along which it has a length of $O(2^j)$ while orthogonal to it its width is bounded by some constant independent of $j$ (see Figure 1.1b). To any reader familiar with the notion of the Fourier transform it should be obvious that the real and Fourier space characterizations are roughly equivalent and that the two lines along which the ridgelet is located in real and Fourier space respectively are orthogonal to each other. In order to have efficient methods that express a given function as a linear combinations of ridgelets, and that transform these coefficients back to the original function, some more assumptions on the Fourier space support of the ridgelets have to be made, but these will be developed in a later chapter.

As was already hinted at, one advantage of the ridgelets is that solutions of the RTE typically can be well approximated by a linear combination of only few ridgelets. Therefore, ridgelets can alleviate the memory and also the compute power problems which are caused by the high dimensionality of the RTE. The other advantage is that there exists a preconditioner for the linear system of equations that arises from a ridgelet discretization of the RTE that has been proven [1] to bound the condition number by some constant independent of the number of ridgelets that are used for discretization. In combination, these two points thus make ridgelets the perfect candidates for the discretization of the RTE.

# 2 Preliminaries

## 2.1 Discrete intervals

Throughout this document, we will be working with functions sampled on equispaced grids over an interval. Therefore, it is useful to have some notation at hand to easily specify such a grid which we named a discrete interval.

**Definition 2.1.1** (Discrete intervals)**.** Let $a, b, c \in \mathbb{R}$ and $a < c$, $\frac{c-a}{b} \in \mathbb{Z}^{\geq 0}$. Then,

$$[a : b : c] := \{a, a + b, ..., c - b, c\}$$

If $b$ is omitted, then $b = 1$ is meant. Both the opening and the closing square brackets can be replaced by parentheses and if done so, the last point at the respective end is excluded from the set.

**Example 2.1.2.** $[0 : 0.5 : 2] = \{0, 0.5, 1, 1.5, 2\}$, whereas $[0 : 0.5 : 2) = \{0, 0.5, 1, 1.5\}$

## 2.2 Sobolev spaces

Sobolev spaces are an important tool to measure the smoothness of a function. For our purposes, we will need a definition which is slightly different from the one usually given.

**Definition 2.2.1** ((Periodic) Sobolev spaces)**.** Let $k \in \mathbb{Z}^{>0}$, $L_x, L_y \in \mathbb{R}^{>0}$ and $\Omega = [0, L_x) \times [0, L_y)$ some rectangular domain. Then, the *Sobolev space* $H^k$ is defined as

$$H^k := \left\{ f \in V \mid \int_\Omega \frac{\partial^{k_x+k_y} f}{\partial^{k_x} x \partial^{k_y} y}\, dx\, dy < \infty \quad \forall k_x, k_y \in \mathbb{Z}^{\geq 0},\, k_x, k_y \leq k \right\}$$

where $V$ is the space of periodic functions $\Omega \to \mathbb{C}$.

We differ from the usual definition in that $k_x, k_y$ run over $k_x, k_y \leq k$ instead of $k_x + k_y \leq k$. Also, for convenience we implemented the condition that our functions be periodic directly into the definition of the Sobolev spaces.

## 2.3 Fourier Transform

Although we expect the reader of this document to be familiar with the notion of the Fourier transform and its basic properties, we will nevertheless repeat them here. The reason for this is that there are at least three different variants which all go by the name of "Fourier transform", and each of these variants has still some subvariants depending

on the sign of the exponent and where the normalizing prefactor goes. This multitude of Fourier transforms often leads to confusion and even errors once results from different conventions are combined. Therefore, the objective of this and the next section is to precisely define the two conventions used in this report and prove that some results known from general Fourier theory still hold in these specific conventions.

**Definition 2.3.1** (Fourier transform)**.** Let $L_x, L_y \in \mathbb{R}^{>0}$, $\Omega = [0, L_x) \times [0, L_y)$ some rectangular domain and $f : \Omega \to \mathbb{C}$ a function. Then, the function $\mathcal{F}[f] : \mathbb{Z}^2 \to \mathbb{C}$ given by

$$\mathcal{F}[f](\hat{x}, \hat{y}) = \frac{1}{L_x L_y} \int_\Omega f(x, y)\, e^{-2\pi i \left(\hat{x}\frac{x}{L_x} + \hat{y}\frac{y}{L_y}\right)}\, dx\, dy$$

is called the *Fourier transform* of $f$.

**Definition 2.3.2** (Inverse Fourier transform)**.** Let $L_x, L_y$ and $\Omega$ be as above and $\hat{f} : \mathbb{Z}^2 \to \mathbb{C}$ a function. Then, the function $\mathcal{F}^{-1}[\hat{f}] : \Omega \to \mathbb{C}$ given by

$$\mathcal{F}^{-1}[\hat{f}](x, y) = \sum_{(\hat{x},\hat{y})\in\mathbb{Z}^2} \hat{f}(\hat{x}, \hat{y})\, e^{2\pi i \left(\hat{x}\frac{x}{L_x} + \hat{y}\frac{y}{L_y}\right)}$$

is called the *inverse Fourier transform* of $\hat{f}$.

Note that $\mathcal{F}^{-1}[\hat{f}](x, y)$ is actually defined for all $(x, y) \in \mathbb{R}^2$ and that $\mathcal{F}^{-1}[\hat{f}](x - n_x L_x, y - n_y L_y) = \mathcal{F}^{-1}[\hat{f}](x, y)$ holds for all $(n_x, n_y) \in \mathbb{Z}^2$. Therefore, the natural domain of definition of $\mathcal{F}^{-1}[\hat{f}]$ would be the periodic extension of $\Omega$ to the whole $\mathbb{R}^2$. When we later deal with translations of real space functions, we will have to assume this point of view for all real space functions $f : \Omega \to \mathbb{C}$ as otherwise an expression of the form $f(x - t_x, y - t_y)$ might not be defined because $(x - t_x, y - t_y)$ lies outside of $\Omega$. However, it would be too tedious to keep repeating that point whenever the need arises, thus in future we will just tacitly assume that whenever a function $f$ is defined as $f : \Omega \to \mathbb{C}$, its actual domain of definition is the periodic extension of $\Omega$ to the whole $\mathbb{R}^2$.

Although important, the following point is somewhat technical and we assume it to be generally known. Therefore, we present it simply as a fact without any proof or reference.

**Fact 2.3.3.** *The Fourier transform and inverse Fourier transform are (essentially) bijective.*

The "essentially" has to be added because the correctness of the above statement depends of course on what function spaces you choose as the domains and ranges of the Fourier transforms. There are some theoretical issues to be considered when choosing these spaces (see e.g. [4, Satz V.2.8] where the above fact is proven for the case of $\Omega = \mathbb{R}^2$), but these theoretical subtleties are of little concern in practice. For the purpose of this report, it is thus good enough to assume that the above fact simply holds for all "reasonable" functions, i.e. functions that appear in a physics related context.

Let us now show that the usage of "inverse" in the Fourier transforms is really justified.

**Theorem 2.3.4** (Inverse property of Fourier transforms)**.** *(Under some weak conditions,) the Fourier transform and inverse Fourier transform are inverse to each other, i.e.* $\mathcal{F} \circ \mathcal{F}^{-1} = \mathcal{F}^{-1} \circ \mathcal{F} = \mathbb{I}$.

*Proof.* Let $L_x, L_y, \Omega$ and $\hat{f}$ be as above. Then,

$$\begin{aligned}
\mathcal{F}[\mathcal{F}^{-1}[\hat{f}]](\hat{x},\hat{y}) &= \frac{1}{L_x L_y} \int_\Omega \left( \sum_{(\hat{v},\hat{w})\in\mathbb{Z}^2} \hat{f}(\hat{v},\hat{w})\, e^{2\pi i\,(\hat{v}\frac{x}{L_x} + \hat{w}\frac{y}{L_y})} \right) e^{-2\pi i\,(\hat{x}\frac{x}{L_x} + \hat{y}\frac{y}{L_y})}\, dx\, dy \\
&= \sum_{(\hat{v},\hat{w})\in\mathbb{Z}^2} \hat{f}(\hat{v},\hat{w})\, \frac{1}{L_x L_y} \int_\Omega e^{2\pi i\,((\hat{v}-\hat{x})\frac{x}{L_x} + (\hat{w}-\hat{y})\frac{y}{L_y})}\, dx\, dy \\
&= \sum_{(\hat{v},\hat{w})\in\mathbb{Z}^2} \hat{f}(\hat{v},\hat{w})\, \delta(\hat{v}-\hat{x})\, \delta(\hat{w}-\hat{y}) \\
&= \hat{f}(\hat{x},\hat{y})
\end{aligned}$$

where in the second line we have assumed that the integral and the series commute.

The other direction, i.e. $\mathcal{F}^{-1} \circ \mathcal{F} = \mathbb{I}$, follows by 2.3.3. □

We conclude this section with three basic results which will be used later.

**Theorem 2.3.5** (Fourier transform of translation)**.** *Let* $L_x, L_y, \Omega$ *be as above and* $f : \Omega \to \mathbb{C}$ *a function with periodic continuation to* $\mathbb{R}^2$*. Then, we have*

$$\mathcal{F}[f(\cdot - t_x, \cdot - t_y)](\hat{x},\hat{y}) = e^{-2\pi i\,(\hat{x}\frac{t_x}{L_x} + \hat{y}\frac{t_y}{L_y})}\, \mathcal{F}[f](\hat{x},\hat{y})$$

*Proof.*

$$\begin{aligned}
\mathcal{F}[f(\cdot - t_x, \cdot - t_y)](\hat{x},\hat{y}) &= \frac{1}{L_x L_y} \int_\Omega f(x - t_x, y - t_y) e^{-2\pi i\,(\hat{x}\frac{x}{L_x} + \hat{y}\frac{y}{L_y})}\, dx\, dy \\
&= \frac{1}{L_x L_y} \int_\Omega f(x,y) e^{-2\pi i\,(\hat{x}\frac{x+t_x}{L_x} + \hat{y}\frac{y+t_x}{L_y})}\, dx\, dy \\
&= e^{-2\pi i\,(\hat{x}\frac{t_x}{L_x} + \hat{y}\frac{t_y}{L_y})}\, \mathcal{F}[f](\hat{x},\hat{y})
\end{aligned}$$

□

**Theorem 2.3.6** (Plancherel formula)**.** *Let* $L_x, L_y, \Omega$ *be as above and* $f, g : \Omega \to \mathbb{C}$*. Then, we have*

$$\int_\Omega f(x,y)\, \overline{g(x,y)}\, dx\, dy = L_x L_y \sum_{(\hat{x},\hat{y})\in\mathbb{Z}^2} \mathcal{F}[f](\hat{x},\hat{y})\, \overline{\mathcal{F}[g](\hat{x},\hat{y})}$$

*Proof.*

$$\begin{aligned}
\int_\Omega f(x,y)\,\overline{g(x,y)}\,dx\,dy &= \int_\Omega \mathcal{F}^{-1}[\mathcal{F}[f]](x,y)\,\overline{\mathcal{F}^{-1}[\mathcal{F}[g]](x,y)}\,dx\,dy \\
&= \int_\Omega \left( \sum_{(\hat{x},\hat{y})\in\mathbb{Z}^2} \mathcal{F}[f](\hat{x},\hat{y})\, e^{2\pi i\,(\hat{x}\frac{x}{L_x}+\hat{y}\frac{y}{L_y})} \right) \dots \\
&\qquad \left( \sum_{(\hat{v},\hat{w})\in\mathbb{Z}^2} \overline{\mathcal{F}[g](\hat{v},\hat{w})}\, e^{-2\pi i\,(\hat{v}\frac{x}{L_x}+\hat{w}\frac{y}{L_y})} \right) dx\,dy \\
&= \sum_{(\hat{x},\hat{y})\in\mathbb{Z}^2} \sum_{(\hat{v},\hat{w})\in\mathbb{Z}^2} \mathcal{F}[f](\hat{x},\hat{y})\,\overline{\mathcal{F}[g](\hat{v},\hat{w})} \int_\Omega e^{2\pi i\,((\hat{x}-\hat{v})\frac{x}{L_x}+(\hat{y}-\hat{w})\frac{y}{L_y})} \\
&= L_x L_y \sum_{(\hat{x},\hat{y})\in\mathbb{Z}^2} \mathcal{F}[f](\hat{x},\hat{y})\,\overline{\mathcal{F}[g](\hat{x},\hat{y})}
\end{aligned}$$

Again, we have assumed that the integral and the series commute. □

**Theorem 2.3.7** (Decay of Fourier coefficients)**.** *Let $L_x, L_y \in \mathbb{R}^{>0}$ and $f : [0, L_x) \times [0, L_y) \to \mathbb{C}$ in the Sobolev space $H^k, k \geq 1$. Then,*

$$\mathcal{F}[f](\hat{x},\hat{y}) = O\left(\frac{1}{\hat{x}^k\hat{y}^k}\right) \quad \text{for } \hat{x},\hat{y} \to \infty$$

*Proof.* By partial integration of the integral over $x$, we get

$$\begin{aligned}
\mathcal{F}[f](\hat{x},\hat{y}) &= \frac{1}{L_x L_y} \int_0^{L_y} \int_0^{L_x} \underbrace{f(x,y)}_{\downarrow} \underbrace{e^{-2\pi i\,(\hat{x}\frac{x}{L_x}+\hat{y}\frac{y}{L_y})}}_{\uparrow}\,dx\,dy \\
&= \frac{1}{L_x L_y} \int_0^{L_y} \left( \underbrace{f(x,y)\frac{-L_x}{2\pi i\hat{x}} e^{-2\pi i\,(\hat{x}\frac{x}{L_x}+\hat{y}\frac{y}{L_y})}\Big|_0^{L_x}}_{=0} \dots \right. \\
&\qquad \left. - \int_0^{L_x} \frac{\partial f}{\partial x}(x,y)\frac{-L_x}{2\pi i\hat{x}} e^{-2\pi i\,(\hat{x}\frac{x}{L_x}+\hat{y}\frac{y}{L_y})}\,dx \right) dy \\
&= \frac{1}{L_y}\frac{1}{2\pi i\hat{x}} \int_0^{L_y} \int_0^{L_x} \frac{\partial f}{\partial x}(x,y) e^{-2\pi i\,(\hat{x}\frac{x}{L_x}+\hat{y}\frac{y}{L_y})}\,dx\,dy
\end{aligned}$$

The underbrace vanishes because the two terms for $x = 0$ and $x = L_x$ are equal as $f$ is assumed to be periodic. By doing the same steps also for $y$, we get

$$\mathcal{F}[f](\hat{x},\hat{y}) = \frac{1}{2\pi i\hat{x}}\frac{1}{2\pi i\hat{y}} \int_0^{L_y} \int_0^{L_x} \frac{\partial^2 f}{\partial x\partial y}(x,y) e^{-2\pi i\,(\hat{x}\frac{x}{L_x}+\hat{y}\frac{y}{L_y})}\,dx\,dy$$

Since $f \in H^k, k \geq 1$, the integrals are bounded, thus

$$\mathcal{F}[f](\hat{x}, \hat{y}) = O\left(\frac{1}{\hat{x}\hat{y}}\right)$$

If $k > 1$, then $\frac{\partial^2 f}{\partial x \partial y} \in H^{k-1}$, thus we can repeat the above steps and eventually get

$$\mathcal{F}[f](\hat{x}, \hat{y}) = O\left(\frac{1}{\hat{x}^k \hat{y}^k}\right)$$

□

## 2.4 Finite Fourier Transform

While the above definition of the Fourier transform provides a solid basis for theoretical work, it is useless if one wants to use it on a finite computing machine because of the integrals and the series. Therefore, what is needed is a finitely computable approximation to the ideal Fourier transform.

**Definition 2.4.1** (Finite Fourier transform)**.** Let $L_x, L_y \in \mathbb{R}^{>0}$, $N_x, N_y \in \mathbb{Z}^{\geq N}$,

$$\Omega_F = \left[0 : \frac{L_x}{N_x} : L_x\right) \times \left[0 : \frac{L_y}{N_y} : L_y\right)$$

an equispaced rectangular grid,

$$\hat{\Omega}_F = \left[-\lceil\frac{N_x - 1}{2}\rceil : \lfloor\frac{N_x - 1}{2}\rfloor\right] \times \left[-\lceil\frac{N_y - 1}{2}\rceil : \lfloor\frac{N_y - 1}{2}\rfloor\right]$$

a part of the Fourier space and $f : \Omega_F \to \mathbb{C}$ a function. Then, the function $\texttt{ft}[f] : \hat{\Omega}_F \to \mathbb{C}$ given by

$$\texttt{ft}[f](\hat{x}, \hat{y}) = \frac{1}{N_x N_y} \sum_{(x,y) \in \Omega_F} f(x, y)\, e^{-2\pi i \left(\hat{x}\frac{x}{L_x} + \hat{y}\frac{y}{L_y}\right)}$$

is called the *finite Fourier transform* of $f$.

It is worth noting that `ft` corresponds to a trapezoidal rule approximation of the integral in the definition of $\mathcal{F}$.

**Definition 2.4.2** (Inverse finite Fourier transform)**.** Let $L_x, L_y$, $N_x, N_y$, $\Omega_F$ and $\hat{\Omega}_F$ as above and $\hat{f} : \hat{\Omega}_F \to \mathbb{C}$ a function. Then, the function $\texttt{ift}[\hat{f}] : \Omega_F \to \mathbb{C}$ given by

$$\texttt{ift}[\hat{f}](x, y) = \sum_{(\hat{x}, \hat{y}) \in \hat{\Omega}_F} \hat{f}(\hat{x}, \hat{y})\, e^{2\pi i \left(\hat{x}\frac{x}{L_x} + \hat{y}\frac{y}{L_y}\right)}$$

is called the *inverse finite Fourier transform* of $\hat{f}$.

Instead of restricting $\texttt{ift}[\hat{f}]$ to $\Omega_F$, the above formula would also allow to define $\texttt{ift}[\hat{f}]$ as a function $[0, L_x) \times [0, L_y) \to \mathbb{C}$. In that case, we would have

$$\texttt{ift}[\hat{f}](x, y) = \mathcal{F}^{-1}[\mathcal{Z}[\hat{f}]] \quad \forall (x, y) \in [0, L_x) \times [0, L_y)$$

where $\mathcal{Z}$ is defined as follows.

**Definition 2.4.3** (Zero padding operator)**.** Let $\hat{\Omega}_F$ and $\hat{f}$ be as in Definition 2.4.2. Then, $\mathcal{Z}[\hat{f}] : \mathbb{Z}^2 \to \mathbb{C}$ is a function defined by

$$\mathcal{Z}[\hat{f}](\hat{x}, \hat{y}) = \begin{cases} \hat{f}(\hat{x}, \hat{y}) & (\hat{x}, \hat{y}) \in \hat{\Omega}_F \\ 0 & \text{otherwise} \end{cases}$$

and the symbol $\mathcal{Z}$ is called the *zero padding operator*.

Later on, we will also need an operator undoing the effect of $\mathcal{Z}$, which for symmetry we introduce already here.

**Definition 2.4.4** (Cutting operator)**.** Let $\hat{\Omega}_F$ be as in Definition 2.4.2, and $\hat{f} : \mathbb{Z}^2 \to \mathbb{C}$. Then, $\mathcal{C}[\hat{f}] : \hat{\Omega}_F \to \mathbb{C}$ is a function defined by

$$\mathcal{C}[\hat{f}](\hat{x}, \hat{y}) = \hat{f}(\hat{x}, \hat{y})$$

and the symbol $\mathcal{C}$ is called the *cutting operator*.

The advantage of defining `ift` the way we did is that only in this case the transform is truly finitely computable and all of the later statements about properties of the finite Fourier transforms are correct. On the other hand, for the purpose of error estimation it will be useful to assume the "continuous" (meaning defined on a non-discrete set) view on the `ift`.

Having defined the finite Fourier transforms, we need to check again that the usage of "inverse" in the inverse finite Fourier transform is really justified.

**Theorem 2.4.5** (Inverse property of finite Fourier transforms)**.** *The finite Fourier transform and inverse finite Fourier transform are inverse to each other, i.e.* $\texttt{ft} \circ \texttt{ift} = \texttt{ift} \circ \texttt{ft} = \mathbb{I}$.

*Proof.* Let $L_x, L_y$, $N_x, N_y$, $\Omega_F$, $\hat{\Omega}_F$ and $\hat{f}$ as above. Then,

$$\begin{aligned}
\texttt{ft}[\texttt{ift}[\hat{f}]](\hat{x}, \hat{y}) &= \frac{1}{N_x N_y} \sum_{(x,y) \in \Omega_F} \left( \sum_{(\hat{v}, \hat{w}) \in \hat{\Omega}_F} \hat{f}(\hat{v}, \hat{w})\, e^{2\pi i \left(\hat{v} \frac{x}{L_x} + \hat{w} \frac{y}{L_y}\right)} \right) e^{-2\pi i \left(\hat{x} \frac{x}{L_x} + \hat{y} \frac{y}{L_y}\right)} \\
&= \sum_{(\hat{v}, \hat{w}) \in \hat{\Omega}_F} \hat{f}(\hat{v}, \hat{w}) \frac{1}{N_x N_y} \sum_{(x,y) \in \Omega_F} e^{2\pi i \left((\hat{v} - \hat{x}) \frac{x}{L_x} + (\hat{w} - \hat{x}) \frac{y}{L_y}\right)} \\
&= \sum_{(\hat{v}, \hat{w}) \in \hat{\Omega}_F} \hat{f}(\hat{v}, \hat{w})\, \delta(\hat{v} - \hat{x})\, \delta(\hat{w} - \hat{y}) \\
&= \hat{f}(\hat{x}, \hat{y})
\end{aligned}$$

The fact that the sums $\frac{1}{N_x N_y} \sum_{(x,y)\in\Omega_F} e^{2\pi i\,((\hat{v}-\hat{x})\frac{x}{L_x}+(\hat{w}-\hat{x})\frac{y}{L_y})}$ collapse to delta functions is a consequence of the summation property of the root of unity:

$$\sum_{k=0}^{N-1} e^{2\pi i\, a\frac{k}{N}} = N\,\delta(a \bmod N), \quad \forall a \in \mathbb{Z}$$

The other direction, i.e. $\texttt{ift} \circ \texttt{ft} = \mathbb{I}$, can be proven in exactly the same way. □

Since the purpose of the finite Fourier transforms is to provide finitely computable approximations to the ideal Fourier transform, it is well worth taking a look at their computational complexity as well as at their approximation properties.

**Theorem 2.4.6** (Complexity of `ft` / `ift`)**.** *Both the finite Fourier transform as well as the inverse finite Fourier transform can be evaluated in all $N_xN_y$ points at once in $O(N_xN_ylog(N_xN_y))$.*

*Proof.* We show how the `ft` can be expressed in terms of a discrete Fourier transform whose complexity is known to be $O(N_xN_y \log(N_xN_y))$. The same argument can be easily applied to the `ift` as well.

$$\begin{aligned}
\texttt{ft}[f](\hat{x},\hat{y}) &= \frac{1}{N_xN_y} \sum_{(x,y)\in\Omega_F} f(x,y) e^{-2\pi i\,(\hat{x}\frac{x}{L_x}+\hat{y}\frac{y}{L_y})} \\
&= \frac{1}{N_xN_y} \sum_{k_x=0}^{N_x-1} \sum_{k_y=0}^{N_y-1} f\left(L_x\frac{k_x}{N_x}, L_y\frac{k_y}{N_y}\right) e^{-2\pi i\,(\hat{x}\frac{k_x}{N_x}+\hat{y}\frac{k_y}{N_y})} \\
&= \frac{1}{N_xN_y} \sum_{k_x=0}^{N_x-1} \sum_{k_y=0}^{N_y-1} F_{k_x,k_y}\, e^{-2\pi i\,(\frac{\hat{x}k_x}{N_x}+\frac{\hat{y}k_y}{N_y})} \\
&= \frac{1}{N_xN_y} \texttt{DFT}[F]
\end{aligned}$$

where $F_{k_x,k_y} := f\left(L_x\frac{k_x}{N_x}, L_y\frac{k_y}{N_y}\right)$. □

The error introduced by the finite Fourier transforms can be split into two parts: One accounts for the fact that we replace the infinite Fourier space $\mathbb{Z}^2$ by some finite subset thereof and will be called the truncation error. The other error is introduced by the fact that we replace the integrals in the ideal Fourier transform by quadrature with the trapezoidal rule, and accordingly we named it the quadrature error.

**Theorem 2.4.7** (Convergence of truncation error)**.** *Let $N \in \mathbb{Z}^{>0}$, $L_x, L_y \in \mathbb{R}^{>0}$ and $f : [0, L_x) \times [0, L_y) \to \mathbb{C}$ in the Sobolev space $H^k, k > 1$. Then,*

$$\sum_{(\hat{x},\hat{y})\in\mathbb{Z}^2\setminus[-N:N]^2} |\mathcal{F}[f](\hat{x},\hat{y})|^2 = O\left(N^{-(2k-1-\varepsilon)}\right)$$

*for any $\varepsilon \in (0, 2k-1)$.*

*Proof.* Using the decay property 2.3.7 of the Fourier coefficients, we get

$$\begin{aligned}\sum_{(\hat{x},\hat{y})\in\mathbb{Z}^2\setminus[-N:N]^2} |\mathcal{F}[f](\hat{x},\hat{y})|^2 &= \sum_{(\hat{x},\hat{y})\in\mathbb{Z}^2\setminus[-N:N]^2} O\left(\frac{1}{\hat{x}^{2k}\hat{y}^{2k}}\right) \\ &= O\left(\sum_{\hat{x}=N+1}^{\infty}\sum_{\hat{y}=1}^{\infty}\frac{1}{\hat{x}^{2k}\hat{y}^{2k}}\right) \\ &= O\left(\sum_{\hat{x}=N+1}^{\infty}\frac{1}{\hat{x}^{2k}}\right)\end{aligned}$$

The sum over $\hat{y}$ can be dropped because $\sum_{\hat{y}=1}^{\infty}\frac{1}{\hat{y}^{2k}}$ with $k > \frac{1}{2}$ is an over-harmonic series and therefore convergent. Choosing some arbitrary $\varepsilon \in (0, 2k-1)$, we further get

$$\begin{aligned}\sum_{(\hat{x},\hat{y})\in\mathbb{Z}^2\setminus[-N:N]^2} |\mathcal{F}[f](\hat{x},\hat{y})|^2 &= O\left(\frac{1}{N^{2k-1-\varepsilon}}\sum_{\hat{x}=N+1}^{\infty}\underbrace{\frac{N^{2k-1-\varepsilon}}{\hat{x}^{2k-1-\varepsilon}}}_{<1}\frac{1}{\hat{x}^{1+\varepsilon}}\right) \\ &= O\left(\frac{1}{N^{2k-1-\varepsilon}}\sum_{\hat{x}=N+1}^{\infty}\frac{1}{\hat{x}^{1+\varepsilon}}\right) \\ &= O\left(\frac{1}{N^{2k-1-\varepsilon}}\right)\end{aligned}$$

In the last line, we made again use of the fact that the over-harmonic series are convergent. □

**Lemma 2.4.8** (Convergence of trapezoidal rule)**.** *Let $L_x, L_y \in \mathbb{R}^{>0}$, $N \in \mathbb{Z}^{>0}$, $\Omega_F := [0 : \frac{L_x}{N} : L_x) \times [0 : \frac{L_y}{N} : L_y)$, $f : [0, L_x) \times [0, L_y) \to \mathbb{C}$ in the Sobolev space $H^k, k > 1$ and*

$$T[f] := \frac{L_x L_y}{N^2}\sum_{(x,y)\in\Omega_F} f(x,y)$$

*the $L_x, L_y$-periodic trapezoidal rule quadrature operator. Then,*

$$T[f] - \int_0^{L_x}\int_0^{L_y} f(x,y)\,dy\,dx = O\left(\frac{1}{N^k}\right)$$

*Proof.* From the definition of $\mathcal{F}$, we get

$$\int_0^{L_x}\int_0^{L_y} f(x,y)\,dy\,dx = L_x L_y \mathcal{F}[f](0,0)$$

On the other hand, inserting $f = \mathcal{F}^{-1}[\mathcal{F}[f]]$ into the definition of $T$, we get

$$\begin{aligned} T[f] &= \frac{L_x L_y}{N_x N_y} \sum_{(x,y)\in\Omega_F} \sum_{(\hat{x},\hat{y})\in\mathbb{Z}^2} \mathcal{F}[f](\hat{x},\hat{y}) e^{2\pi i \left(\hat{x}\frac{x}{L_x} + \hat{y}\frac{y}{L_y}\right)} \\ &= L_x L_y \sum_{(\hat{x},\hat{y})\in\mathbb{Z}^2} \mathcal{F}[f](\hat{x},\hat{y})\, \delta\left(\hat{x} \bmod N\right) \delta\left(\hat{y} \bmod N\right) \\ &= L_x L_y \sum_{(\hat{x},\hat{y})\in\mathbb{Z}^2} \mathcal{F}[f](N\hat{x}, N\hat{y}) \end{aligned}$$

The error is thus

$$T[f] - \int_0^{L_x}\int_0^{L_y} f(x,y)\,dy\,dx = L_x L_y \left( \sum_{(\hat{x},\hat{y})\in\mathbb{Z}^2} \mathcal{F}[f](N\hat{x}, N\hat{y}) - \mathcal{F}[f](0,0) \right)$$

Combining this result with the decay property 2.3.7 of the Fourier coefficients, the estimate immediately follows.

The key ideas of this proof were taken from [7, Section 3]. □

**Theorem 2.4.9** (Convergence of quadrature error)**.** *Let $N \in \mathbb{Z}^{>0}$, $L_x, L_y \in \mathbb{R}^{>0}$ and $f : [0, L_x) \times [0, L_y) \to \mathbb{C}$ in the Sobolev space $H^k, k > 1$. Furthermore, let the number of finite Fourier transform grid points be $N_x = N_y = N$. Then,*

$$\sum_{(\hat{x},\hat{y})\in[-N:N]^2} |\mathcal{F}[f](\hat{x},\hat{y}) - \mathtt{ft}[f](\hat{x},\hat{y})|^2 = O\left(N^{-2(k-1)}\right)$$

*Proof.* By the above Lemma 2.4.8, we get

$$\begin{aligned} \sum_{(\hat{x},\hat{y})\in[-N:N]^2} |\mathcal{F}[f](\hat{x},\hat{y}) - \mathtt{ft}[f](\hat{x},\hat{y})|^2 &= \sum_{(\hat{x},\hat{y})\in[-N:N]^2} O\left(\frac{1}{N^k}\right)^2 \\ &= O\left(\frac{1}{N^{2(k-1)}}\right) \end{aligned}$$

□

# 3 Ridgelets

In the introduction, a vague idea was given of what ridgelets are and what they can be used for. In this chapter, we will further clarify these concepts by explicitly constructing a set of ridgelets. Furthermore, we will show that any function can be expressed as a linear combination of these ridgelets without loss of information. Finally, efficient methods will be presented which allow to switch from an explicit representation of a function to its representation as a linear combination of ridgelets and vice versa.

Many ideas in this chapter are taken from [2] and [1].

## 3.1 Construction

Our construction of the ridgelets is parametrized by two functions $\psi_{Radial}$ and $\psi_{Spherical}$ which are introduced in the following two definitions.

**Definition 3.1.1** (Radial shape and helper functions)**.** Let $\psi_{Radial} : [0,1] \to [0,1]$ be a function called *radial shape function*. Then, we define the *radial helper function* $R(x)$ as

$$R(x) := \begin{cases} 0 & |x| \leq 0.5 \\ \psi_{Radial}(2x-1) & 0.5 < |x| < 1 \\ 1 & |x| = 1 \\ \sqrt{1 - \psi_{Radial}(x-1)^2} & 1 < |x| < 2 \\ 0 & 2 \leq |x| \end{cases}$$

**Definition 3.1.2** (Spherical shape and helper functions)**.** Let $\psi_{Spherical} : [0,1] \to [0,1]$ be a function called *spherical shape function*. Then, we define the *spherical helper function* $\Phi(x)$ as

$$\Phi(x) := \begin{cases} 0 & x \leq -1 \\ \sqrt{1 - \psi_{Spherical}(x+1)^2} & -1 < x < 0 \\ 1 & x = 0 \\ \psi_{Spherical}(x) & 0 < x < 1 \\ 0 & 1 \leq x \end{cases}$$

Although not strictly necessary for the results shown here, the helper functions are usually chosen as continuous and monotonous functions with

$$\begin{aligned} \psi_{Radial}(0) = 0, \quad \psi_{Radial}(1) = 1 \\ \psi_{Spherical}(0) = 1, \quad \psi_{Spherical}(1) = 0 \end{aligned}$$

With these helper functions at hand, we can start defining our ridgelets.

**Definition 3.1.3** (Basic ridgelet)**.** Let $\rho_x, \rho_y \in \mathbb{Z}^{\geq 1}$ and $\Omega = [0, L_x) \times [0, L_y)$ some rectangular domain. Then, the *basic ridgelet* $\hat{\psi}_{(1,\mathtt{x},0)} : \mathbb{Z}^2 \to [0,1]$ is a function defined in Fourier space by

$$\hat{\psi}_{(1,\mathtt{x},0)}(\hat{x}, \hat{y}) := R\left(\frac{\hat{x}}{2\rho_x}\right) \Phi\left(\frac{\rho_x \hat{y}}{\rho_y \hat{x}}\right)$$

with corresponding real space function $\psi_{(1,\mathtt{x},0)} : \Omega \to \mathbb{C}$ given by

$$\psi_{(1,\mathtt{x},0)} := \mathcal{F}^{-1}[\hat{\psi}_{(1,\mathtt{x},0)}]$$

**Definition 3.1.4** (x-cone ridgelets)**.** Let $\Omega$ be as above. Then, the x-cone ridgelets are a family of functions $\hat{\psi}_{(j,\mathtt{x},k)} : \mathbb{Z}^2 \to [0,1]$ parametrized by $j \in \mathbb{Z}^{\geq 1}$ and $k \in [-2^{j-1} + 1 : 2^{j-1} - 1]$ defined in Fourier space by

$$\hat{\psi}_{(j,\mathtt{x},k)}(\hat{x}, \hat{y}) := \hat{\psi}_{(1,\mathtt{x},0)}\left(\frac{\hat{x}}{2^{j-1}},\, \hat{y} - \frac{k}{2^{j-1}}\hat{x}\right),$$

and with corresponding real space functions $\psi_{(j,\mathtt{x},k)} : \Omega \to \mathbb{C}$ given by

$$\psi_{(j,\mathtt{x},k)} := \mathcal{F}^{-1}[\hat{\psi}_{(j,\mathtt{x},k)}]$$

Note that the x-cone ridgelets correspond to a scaling (in x-direction) with subsequent shearing (in y-direction) of the basic ridgelet. Since we want our ridgelets to cover all directions, we also need some y-cone ridgelets which are defined as the transposed of the x-cone ridgelets.

**Definition 3.1.5** (y-cone ridgelets)**.** The y-cone ridgelets are a family of functions $\hat{\psi}_{(j,\mathtt{y},k)} : \mathbb{Z}^2 \to [0,1]$ parametrized by $j \in \mathbb{Z}^{\geq 1}$ and $k \in [-2^{j-1} + 1 : 2^{j-1} - 1]$ defined in Fourier space by

$$\hat{\psi}_{(j,\mathtt{y},k)}(\hat{x}, \hat{y}) := \hat{\psi}_{(j,\mathtt{x},k)}(\hat{y}, \hat{x}),$$

and with corresponding real space functions $\psi_{(j,\mathtt{y},k)} : \Omega \to \mathbb{C}$ given by

$$\psi_{(j,\mathtt{y},k)} := \mathcal{F}^{-1}[\hat{\psi}_{(j,\mathtt{y},k)}]$$

Finally, in order to have a "continuous" (in a non-mathematical sense) transition between the x- and y-cone ridgelets, we define diagonal ridgelets as a patching of the outermost ridgelets on the cones.

**Definition 3.1.6** (Diagonal ridgelets)**.** Let $\rho_x, \rho_y$ and $\Omega$ be as above. Then, the diagonal ridgelets are a family of functions $\hat{\psi}_{(j,\mathtt{d},k)} : \mathbb{Z}^2 \to [0,1]$ parametrized by $j \in \mathbb{Z}^{\geq 1}$ and $k \in \{-1, 1\}$ defined in Fourier space by

$$\hat{\psi}_{(j,\mathtt{d},k)}(\hat{x}, \hat{y}) := \begin{cases} \hat{\psi}_{(j,\mathtt{x},k\,2^{j-1})}(\hat{x}, \hat{y}) & \frac{|\hat{x}|}{\rho_x} \geq \frac{|\hat{y}|}{\rho_y} \\ \hat{\psi}_{(j,\mathtt{y},k\,2^{j-1})}(\hat{x}, \hat{y}) & \frac{|\hat{x}|}{\rho_x} < \frac{|\hat{y}|}{\rho_y} \end{cases}$$

and with corresponding real space functions $\psi_{(j,\mathtt{d},k)} : \Omega \to \mathbb{C}$ given by

$$\psi_{(j,\mathtt{d},k)} := \mathcal{F}^{-1}[\hat{\psi}_{(j,\mathtt{d},k)}]$$

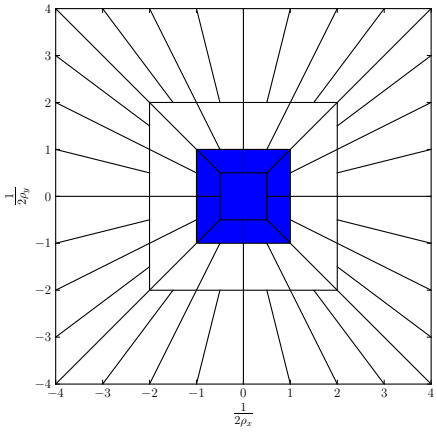


(a) Scaling function $\hat{\psi}_{(0,\mathtt{s},0)}$

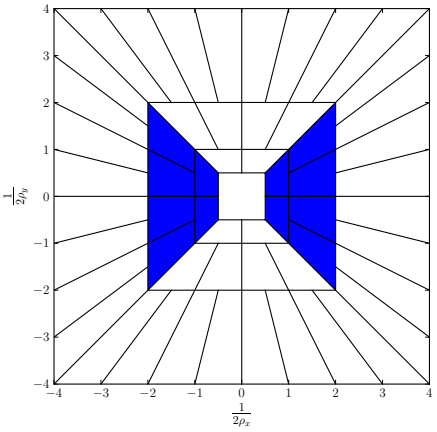


(b) Basic ridgelet $\hat{\psi}_{(1,\mathtt{x},0)}$

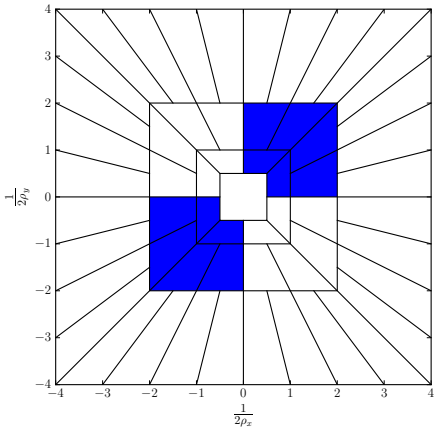


(c) Diagonal ridgelet $\hat{\psi}_{(1,\mathtt{d},1)}$

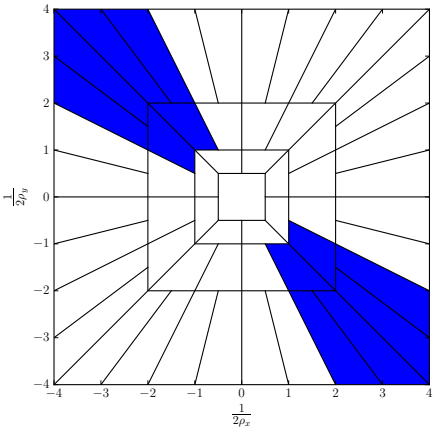


(d) Diagonal ridgelet $\hat{\psi}_{(2,\mathtt{d},-1)}$

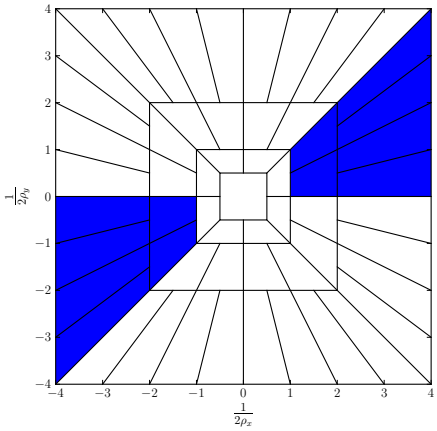


(e) x-cone ridgelet $\hat{\psi}_{(2,\mathtt{x},1)}$

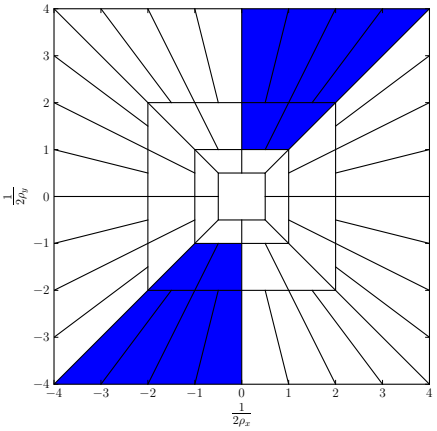


(f) y-cone ridgelet $\hat{\psi}_{(2,\mathtt{y},1)}$

Figure 3.1: Fourier space supports of several ridgelets

(Actually, $k\,2^{j-1}$ lies outside the domain of the shear parameter $k$ for $\kappa \in \{\mathtt{x}, \mathtt{y}\}$. Reconsidering Definition 3.1.4 it is nevertheless clear what the meaning of $\hat{\psi}_{(j,\kappa,k\,2^{j-1})}$ is, however.)

With the ridgelets defined so far, we cover all directions. However, we still need some function that covers the low frequency part (which corresponds to the mass of the function in real space).

**Definition 3.1.7** (Scaling function)**.** Given $\rho_x, \rho_y$ and $\Omega$ as above, the *scaling function* $\hat{\psi}_{(0,\mathtt{s},0)} : \mathbb{Z}^2 \to [0,1]$ is a function defined in Fourier space by

$$\hat{\psi}_{(0,\mathtt{s},0)}(\hat{x},\hat{y}) := \begin{cases} 1 & s < \frac{1}{2} \\ \sqrt{1 - \psi_{Radial}(2s-1)^2} & \frac{1}{2} \le s < 1 \\ 0 & 1 \le s \end{cases} \quad \text{with } s := \max\left\{ \frac{|\hat{x}|}{2\rho_x}, \frac{|\hat{y}|}{2\rho_y} \right\}$$

with corresponding real space function $\psi_{(0,\mathtt{s},0)} : \Omega \to \mathbb{C}$ given by

$$\psi_{(0,\mathtt{s},0)} := \mathcal{F}^{-1}[\hat{\psi}_{(0,\mathtt{s},0)}]$$

With the scaling function, the set of ridgelets is now complete. In the remainder of this chapter, it will become clear that the most important property of a ridgelet is its well-defined support in the Fourier space. Unfortunately, giving a lucid description of what these supports look like in words or formulae is almost impossible. Therefore, we rather refer the reader to the examples given in Figure 3.1, following the ancient wisdom that at times, pictures can say more than a thousand words.

As the attentive reader noticed, the ridgelets are parametrized by a triple $(j, \kappa, k)$ of variables which tell us about the length and the direction of the respective ridgelet. Often, however, we are not interested in such details and simply want to specify that we mean *all* of the above defined ridgelets. For this purpose, the following set comes in useful.

**Definition 3.1.8** (Index set)**.** The *index set* $\Lambda$ is defined as the set of all triples

$$\lambda = \begin{cases} (j = 0, \kappa = \mathtt{s}, k = 0) \\ (j \in \mathbb{Z}^{\ge 1}, \kappa \in \{\mathtt{x}, \mathtt{y}\}, k \in [-2^{j-1} + 1 : 2^{j-1} - 1]) \\ (j \in \mathbb{Z}^{\ge 1}, \kappa = \mathtt{d}, k \in \{-1, 1\}) \end{cases}$$

$j$ is called the *scale parameter*, $\kappa$ the *direction parameter* and $k$ the *shear parameter*.

The following lemma is a first example of the usefulness of having such a set $\Lambda$.

**Lemma 3.1.9** (Partition of unity)**.** *The $\hat{\psi}_\lambda$ with $\lambda \in \Lambda$ constitute a partition of unity, i.e.*

$$\sum_{\lambda \in \Lambda} \hat{\psi}_\lambda^2(\hat{x},\hat{y}) = 1 \quad \forall (\hat{x},\hat{y}) \in \mathbb{Z}^2$$

*Proof.* We will not give a complete proof here as doing so would be very tedious and give little insight. Rather, we will settle for the main points.

First, note that $\Phi^2(x) + \Phi^2(x-1) = 1$ for all $x \in [0,1]$. Therefore, we have that e.g.

$$\hat{\psi}^2_{(j,\mathtt{x},k)}(\hat{x},\hat{y}) + \hat{\psi}^2_{(j,\mathtt{x},k+1)}(\hat{x},\hat{y}) = R^2\left(\frac{|\hat{x}|}{\rho_x 2^j}\right)$$

for all $(\hat{x},\hat{y}) \in \operatorname{supp}\hat{\psi}_{(j,\mathtt{x},k)} \cap \operatorname{supp}\hat{\psi}_{(j,\mathtt{x},k+1)}$. If we extend this argument to all ridgelets on the same scale $j$, we see that the dependence on the spherical part $\Phi$ completely drops out and that we are left with only the radial part $R$. But since we have that $R^2(x) + R^2(\frac{x}{2}) = 1$ for all $x \in [-2,-1] \cup [1,2]$, this part will become a 1 once we square and sum over all scales $j \in \mathbb{Z}^{\geq 0}$. □

As in [2] and [1], this partition of unity property of the ridgelets will be the key point in proving the invertibility of the ridgelet transform in 3.2.8.

In the introduction, we specified the ridgelets as a set of functions with varying locations, directions and width. So far, we have only covered the direction and width. Next, we will thus have a look at the translations of the ridgelets.

**Definition 3.1.10** (Translation sets)**.** Let $\rho_x, \rho_y$ and $\Lambda$ be as above. Then, the *translation sets* $T^\lambda$ with $\lambda \in \Lambda$ are defined as

$$T^\lambda := \begin{cases} [0 : \frac{L_x}{4\rho_x} : L_x) \times [0 : \frac{L_y}{4\rho_y} : L_y) & \text{if } \kappa = \mathtt{s} \\ [0 : \frac{L_x}{2^{j+2}\rho_x} : L_x) \times [0 : \frac{L_y}{8\rho_y} : L_y) & \text{if } \kappa = \mathtt{x} \\ [0 : \frac{L_x}{8\rho_x} : L_x) \times [0 : \frac{L_y}{2^{j+2}\rho_y} : L_y) & \text{if } \kappa = \mathtt{y} \\ [0 : \frac{L_x}{2^{j+2}\rho_x} : L_x) \times [0 : \frac{L_y}{8\rho_y} : L_y) & \text{if } \kappa = \mathtt{d} \end{cases}$$

Furthermore, we define

$$T^\lambda_x := \begin{cases} 4\rho_x & \text{if } \kappa = \mathtt{s} \\ 2^{j+2}\rho_x & \text{if } \kappa = \mathtt{x} \\ 8\rho_x & \text{if } \kappa = \mathtt{y} \\ 2^{j+2}\rho_x & \text{if } \kappa = \mathtt{d} \end{cases} \quad \text{and} \quad T^\lambda_y := \begin{cases} 4\rho_y & \text{if } \kappa = \mathtt{s} \\ 8\rho_y & \text{if } \kappa = \mathtt{x} \\ 2^{j+2}\rho_y & \text{if } \kappa = \mathtt{y} \\ 8\rho_y & \text{if } \kappa = \mathtt{d} \end{cases}$$

We conclude this section by collecting all the defined functions in a set.

**Definition 3.1.11** (Ridgelet frame)**.** The set of functions

$$\{\psi_\lambda\}_{\Lambda,T^\lambda} := \{\psi_\lambda(\cdot - t_x, \cdot - t_y) \,|\, \lambda \in \Lambda,\, t \in T^\lambda\}$$

is called a *ridgelet frame*.

The reasons for this set to be called a frame is that the (rescaled) $\{\psi_\lambda\}_{\Lambda,T^\lambda}$ satisfy the frame condition

$$\|f\|_2^2 \sim \sum_{\lambda\in\Lambda}\sum_{t\in T^\lambda} \langle f,\, \psi_\lambda(\cdot - t_x, \cdot - t_y)\rangle_2$$

where $f : \Omega \to \mathbb{C}$ is some arbitrary function and the $\sim$ means that the left side is bounded by a constant times the right side and vice versa. In this report, no further reference to this frame property will be made, however.

## 3.2 Ridgelet Transform

In analogy to the Fourier transforms, the process of expressing a given function as a linear combination of ridgelets is called a ridgelet transform, and the opposite operation an inverse ridgelet transform. These transforms introduce a new space of linear combination coefficients which is called the ridgelet coefficient space.

**Definition 3.2.1** (Ridgelet coefficient space)**.** The set of pairs

$$(\Lambda, T) := \{(\lambda, t) \,|\, \lambda \in \Lambda,\, t \in T^\lambda\}$$

is called the *ridgelet coefficient space*.

**Definition 3.2.2** (Ridgelet transform)**.** Let $\Omega = [0, L_x) \times [0, L_y)$ some rectangular domain and $f : \Omega \to \mathbb{C}$ a function. Then, the function $\mathcal{R}[f] : (\Lambda, T) \to \mathbb{C}$ given by

$$\mathcal{R}[f](\lambda, t) := \frac{1}{L_x L_y} \frac{1}{T_x^\lambda T_y^\lambda} \int_\Omega f(x, y)\, \overline{\psi_\lambda(x - t_x, y - t_y)}\, dx\, dy$$

is called the *ridgelet transform* of $f$.

**Definition 3.2.3** (Inverse ridgelet transform)**.** Let $\Omega = [0, L_x) \times [0, L_y)$ be some rectangular domain and $\tilde{f} : (\Lambda, T) \to \mathbb{C}$ a function. Then, the function $\mathcal{R}^{-1}[\tilde{f}] : \Omega \to \mathbb{C}$ given by

$$\mathcal{R}^{-1}[\tilde{f}](x, y) := \sum_{\lambda \in \Lambda} \sum_{t \in T^\lambda} \tilde{f}(\lambda, t)\, \psi_\lambda(x - t_x, y - t_y)$$

is called the *inverse ridgelet transform* of $f$.

The real space ridgelet transforms as given above show what the idea behind these transforms is. For both theoretical work as well as implementation, it is more useful to work with their Fourier transforms, however.

**Definition 3.2.4** (Fourier ridgelet transform)**.** Let $\hat{f} : \mathbb{Z}^2 \to \mathbb{C}$ be a function. Then, the function $\hat{\mathcal{R}}[\hat{f}] : (\Lambda, T) \to \mathbb{C}$ given by

$$\hat{\mathcal{R}}[\hat{f}](\lambda, t) := \mathcal{R}[\mathcal{F}^{-1}[\hat{f}]](\lambda, t)$$

is called the *Fourier ridgelet transform* of $\hat{f}$.

**Theorem 3.2.5.** *The Fourier ridgelet transform is given by*

$$\hat{\mathcal{R}}[\hat{f}](\lambda, t) = \frac{1}{T_x^\lambda T_y^\lambda} \sum_{(\hat{x}, \hat{y}) \in \mathbb{Z}^2} \hat{f}(\hat{x}, \hat{y}) \hat{\psi}_\lambda(\hat{x}, \hat{y}) e^{2\pi i \left(\hat{x} \frac{t_x}{L_x} + \hat{y} \frac{t_y}{L_y}\right)}$$

*Proof.* Direct consequence of the Plancherel formula 2.3.6, the translation property of the Fourier transform 2.3.5 and the fact that the ridgelets $\hat{\psi}_\lambda$ are real. □

**Definition 3.2.6** (Inverse Fourier ridgelet transform)**.** Let $\hat{f} : (\Lambda, T) \to \mathbb{C}$ be a function. Then, the function $\hat{\mathcal{R}}^{-1}[\tilde{f}] : \mathbb{Z}^2 \to \mathbb{C}$ given by

$$\hat{\mathcal{R}}^{-1}[\tilde{f}](\hat{x}, \hat{y}) := \mathcal{F}[\mathcal{R}^{-1}[\tilde{f}]](\hat{x}, \hat{y})$$

is called the *inverse Fourier ridgelet transform* of $\tilde{f}$.

**Theorem 3.2.7.** *The inverse Fourier ridgelet transform is given by*

$$\hat{\mathcal{R}}^{-1}[\tilde{f}](\hat{x}, \hat{y}) = \sum_{\lambda \in \Lambda} \sum_{t \in T^\lambda} \tilde{f}(\lambda, t) \hat{\psi}_\lambda(\hat{x}, \hat{y}) e^{-2\pi i \left(\hat{x} \frac{t_x}{L_x} + \hat{y} \frac{t_y}{L_y}\right)}$$

*Proof.* Direct consequence of the linearity of the Fourier transform and the translation property 2.3.5. □

Thanks to this Fourier ridgelet transforms, we are now able to prove the first main theorem of this bachelor thesis.

**Theorem 3.2.8** (Inverse property of the Fourier ridgelet transforms)**.** *The inverse Fourier ridgelet transform is the left inverse of the Fourier ridgelet transform, i.e.* $\hat{\mathcal{R}}^{-1} \circ \hat{\mathcal{R}} = \mathbb{I}$

*Proof.* Let $\hat{f} : \mathbb{Z}^2 \to \mathbb{C}$. Then,

$$\begin{aligned}
\hat{\mathcal{R}}^{-1}[\hat{\mathcal{R}}[\hat{f}]](\hat{x}, \hat{y}) &= \dots \\
&= \sum_{\lambda \in \Lambda} \sum_{t \in T^\lambda} \frac{1}{T_x^\lambda T_y^\lambda} \sum_{(\hat{v}, \hat{w}) \in \mathbb{Z}^2} \hat{f}(\hat{v}, \hat{w}) \, \hat{\psi}_\lambda(\hat{v}, \hat{w}) \, \hat{\psi}_\lambda(\hat{x}, \hat{y}) e^{2\pi i \left((\hat{v} - \hat{x}) \frac{t_x}{L_x} + (\hat{w} - \hat{y}) \frac{t_y}{L_y}\right)} \\
&= \sum_{\lambda \in \Lambda} \sum_{(\hat{v}, \hat{w}) \in \mathbb{Z}^2} \hat{f}(\hat{v}, \hat{w}) \, \hat{\psi}_\lambda(\hat{v}, \hat{w}) \, \hat{\psi}_\lambda(\hat{x}, \hat{y}) \frac{1}{T_x^\lambda T_y^\lambda} \sum_{t \in T^\lambda} e^{2\pi i \left((\hat{v} - \hat{x}) \frac{t_x}{L_x} + (\hat{w} - \hat{y}) \frac{t_y}{L_y}\right)} \\
&= \sum_{\lambda \in \Lambda} \sum_{(\hat{v}, \hat{w}) \in \mathbb{Z}^2} \hat{f}(\hat{v}, \hat{w}) \, \hat{\psi}_\lambda(\hat{v}, \hat{w}) \, \hat{\psi}_\lambda(\hat{x}, \hat{y}) \, \delta\left((\hat{v} - \hat{x}) \bmod T_x^\lambda\right) \, \delta\left((\hat{w} - \hat{y}) \bmod T_y^\lambda\right)
\end{aligned}$$

As in 2.4.5, the fact that $\frac{1}{T_x^\lambda T_y^\lambda} \sum_{t \in T^\lambda} e^{2\pi i \left((\hat{v} - \hat{x}) \frac{t_x}{L_x} + (\hat{w} - \hat{y}) \frac{t_y}{L_y}\right)}$ collapses to delta functions is due to the summation property of the root of unity.

Here we see the reason for the somewhat peculiar choice of $T_x^\lambda$ and $T_y^\lambda$ in 3.1.10: They were chosen such that if $(\hat{x}, \hat{y}) \in \mathbb{Z}^2$ lies in the support of $\hat{\psi}_\lambda$, then all $(\hat{x} - n_x T_x^\lambda, \hat{y} - n_y T_y^\lambda), (n_x, n_y) \in \mathbb{Z}^2 \setminus \{(0, 0)\}$ do not. Therefore, we do not have to bother about the moduli in the delta functions and can instead just write

$$\begin{aligned}
\hat{\mathcal{R}}^{-1}[\hat{\mathcal{R}}[\hat{f}]](\hat{x}, \hat{y}) &= \sum_{\lambda \in \Lambda} \hat{f}(\hat{x}, \hat{y}) \, \hat{\psi}_\lambda^2(\hat{x}, \hat{y}) \\
&= \hat{f}(\hat{x}, \hat{y})
\end{aligned}$$

due to the partition of unity property 3.1.9 of the ridgelets. □

The above theorem implies that the Fourier ridgelet transform is injective and that the inverse Fourier ridgelet transform is surjective. However, it is important to stress that neither of them is bijective! An easy way to see this is to think about what happens if you Fourier ridgelet transform a ridgelet $\hat{\psi}_\lambda$: Obviously, we have $\hat{\mathcal{R}}^{-1}[\tilde{f}] = \hat{\psi}_\lambda$ if we let $\tilde{f}(\mu, t) := \delta(\mu - \lambda)\,\delta(t)$ (here, $\mu - \lambda$ for $\mu, \lambda \in \Lambda$ is defined as zero iff $\mu = \lambda$ and anything different from zero otherwise). But $\tilde{f}$ is not the function produced by $\hat{\mathcal{R}}[\hat{\psi}_\lambda]$! Rather, since $\hat{\psi}_\lambda$ overlaps with some other ridgelets $\hat{\psi}_\mu$ in Fourier space, these $\hat{\psi}_\mu$ will have nonzero coefficients as well. In conclusion, we thus observe the following:

**Fact 3.2.9.** *The Fourier ridgelet transform is not surjective. The inverse Fourier ridgelet transform is not injective.*

Of course, both results hold equally for the original real space ridgelet transforms.

**Corollary 3.2.10** (Inverse property of the ridgelet transforms)**.** *The inverse ridgelet transform is the left inverse of the ridgelet transform, i.e.* $\mathcal{R}^{-1} \circ \mathcal{R} = \mathbb{I}$

*Proof.* By the definition of the (inverse) Fourier ridgelet transform 3.2.4 / 3.2.6 and the inverse property of the Fourier transforms 2.3.4, we can write $\mathcal{R} = \hat{\mathcal{R}} \circ \mathcal{F}$ and $\mathcal{R}^{-1} = \mathcal{F}^{-1} \circ \hat{\mathcal{R}}^{-1}$. Then, the claim follows by the inverse property of the Fourier transforms 2.3.4 and the above theorem. □

**Fact 3.2.11.** *The ridgelet transform is not surjective. The inverse ridgelet transform is not injective.*

## 3.3 Finite Ridgelet Transform

In the same way as we introduced the finite Fourier transform as finitely computable approximations to the ideal Fourier transforms, we will introduce here the finite ridgelet transforms as approximations to the ideal ridgelets transforms defined in the previous section. Since the formulae for the Fourier ridgelet transform already contain only series and sums, we only have to specify how we truncate the series.

**Definition 3.3.1** (Finite index set)**.** Let $J_x, J_y \in \mathbb{Z}^{\geq 1}$. Then the *finite index set* $\Lambda_F$ is given by

$$\Lambda_F^{(J)} = \{\lambda \in \Lambda \,|\, j \leq J\}$$

if $J_x = J_y = J$, and

$$\Lambda_F = \left\{ \lambda \in \Lambda_F^{(J)} \;\middle|\; \begin{cases} \texttt{true} & \text{if } \kappa = \texttt{s} \\ j \leq \min\{J_x, J_y\} + 1 & \text{if } \kappa = \texttt{d} \\ |k| \leq 2^{J_y} & \text{if } \kappa = \texttt{x} \\ |k| \leq 2^{J_x} & \text{if } \kappa = \texttt{y} \end{cases} \right\}$$

where $J = \max\{J_x, J_y\}$ otherwise.

**Definition 3.3.2** (Finite ridgelet coefficient space)**.** The set of pairs

$$(\Lambda_F, T) := \{(\lambda, t) \,|\, \lambda \in \Lambda_F,\, t \in T^\lambda\}$$

is called the *finite ridgelet coefficient space*.

**Definition 3.3.3** (Finite ridgelet transform)**.** Let

$$\hat{\Omega}_F = \begin{cases} [-\rho_x\, 2^{J_{max}+1} : \rho_x\, 2^{J_{max}+1} - 1] \times [-\rho_y\, 2^{J_{max}+1} : \rho_y\, 2^{J_{max}+1} - 1] & \text{if } |J_x - J_y| \leq 1 \\ [-4\rho_x\, (2^{J_x} + 1) : 4\rho_x\, (2^{J_x} + 1) - 1] \times [-\rho_y\, 2^{J_y+1} : \rho_y\, 2^{J_y+1} - 1] & \text{if } J_x < J_y - 1 \\ [-\rho_x\, 2^{J_x+1} : \rho_x\, 2^{J_x+1} - 1] \times [-4\rho_y\, (2^{J_y} + 1) : 4\rho_y\, (2^{J_y} + 1) - 1] & \text{if } J_y < J_x - 1 \end{cases}$$

where $J_{max} := \max\{J_x, J_y\}$ be a part of the Fourier space and $\hat{f} : \hat{\Omega}_F \to \mathbb{C}$ a function. Then, the function $\mathtt{rt}[\hat{f}] : (\Lambda_F, T) \to \mathbb{C}$ given by

$$\mathtt{rt}[\hat{f}](\lambda, t) = \frac{1}{T_x^\lambda T_y^\lambda} \sum_{(\hat{x},\hat{y}) \in \hat{\Omega}_F} \hat{f}(\hat{x}, \hat{y})\, \hat{\psi}_\lambda(\hat{x}, \hat{y})\, e^{2\pi i\, (\hat{x}\frac{t_x}{L_x} + \hat{y}\frac{t_y}{L_y})}$$

is called the *finite (Fourier) ridgelet transform* of $\hat{f}$.

**Definition 3.3.4** (Finite inverse ridgelet transform)**.** Let $\hat{\Omega}_F$ be as above and $\tilde{f} : (\Lambda_F, T) \to \mathbb{C}$ a function. Then, the function $\mathtt{irt}[\tilde{f}] : \hat{\Omega}_F \to \mathbb{C}$ given by

$$\mathtt{irt}[\hat{f}](\hat{x}, \hat{y}) = \sum_{\lambda \in \Lambda_F} \sum_{t \in T^\lambda} \tilde{f}(\lambda, t)\, \hat{\psi}_\lambda(\hat{x}, \hat{y})\, e^{-2\pi i\, (\hat{x}\frac{t_x}{L_x} + \hat{y}\frac{t_y}{L_y})}$$

is called the *finite inverse (Fourier) ridgelet transform* of $\hat{f}$.

Remember from the proof of 3.2.8 that the invertibility of the ridgelet transforms depends on the partition of unity property of the underlying frame. Thus, the following lemma directly tells us on what region we have $\mathtt{irt}[\mathtt{rt}[\hat{f}]] = \hat{f}$.

**Lemma 3.3.5** (Finite partition of unity)**.** *The $\hat{\psi}_\lambda$ with $\lambda \in \Lambda_F$ constitute a partition of unity on a part of $\mathbb{Z}^2$, namely*

$$\sum_{\lambda \in \Lambda_F} \hat{\psi}_\lambda^2(\hat{x}, \hat{y}) = 1 \quad \forall (\hat{x}, \hat{y}) \in [-\rho_x 2^{J_x} : \rho_x 2^{J_x}] \times [-\rho_y 2^{J_y} : \rho_y 2^{J_y}]$$

*Proof.* Analogous to the proof of the partition of unity property 3.1.9 of the ideal ridgelet frame. □

Note that the finite Fourier space $\hat{\Omega}_F$ defined by the finite ridgelet transforms is larger than the region $\hat{\Omega}_1$ where the ridgelets in the finite frame constitute a partition of unity. In principle, one could cut $\hat{\Omega}_F$ to make it equal to $\hat{\Omega}_1$, but this would require special treatment of the ridgelets on scales $j \geq \min\{J_x, J_y\}$ and thus introduce a lot of technical complications. Furthermore, in the current definition the finite ridgelet transforms still conserves *some* of the information in $\hat{\Omega}_F \backslash \hat{\Omega}_1$, and thus the additional effort is not completely wasted.

From Fact 3.2.9 we know that there exists a certain redundancy in the ridgelet coefficient space. The following result allows us to quantify this redundancy.

**Theorem 3.3.6** (Cardinality of finite ridgelet coefficient space)**.**

$$|(\Lambda_F, T)| = \rho_x \rho_y \left(16 + 256\,\frac{4^{J_{min}} - 1}{3} + 64\,(2^{J_{min}+1} + 1)\,(2^{J_{max}} - 2^{J_{min}})\right)$$

*with* $J_{max} = \max\{J_x, J_y\}$ *and* $J_{min} = \min\{J_x, J_y\}$

*Proof.* Sum $T_x^\lambda T_y^\lambda$ for all $\lambda \in \Lambda_F$. □

We see that if $J_{min} = J_{max}$, the redundancy $\frac{|(\Lambda_F,T)|}{|\Omega_1|}$ is bounded by $\frac{64}{3}$ and $\frac{|(\Lambda_F,T)|}{|\Omega_F|}$ by $\frac{16}{3}$. If we drop that condition, we have $\frac{|(\Lambda_F,T)|}{|\Omega_1|} \leq 32$ and $\frac{|(\Lambda_F,T)|}{|\Omega_F|} \leq 8$.

The rest of this section will be dedicated to showing how the finite ridgelet transforms can be evaluated efficiently. The bottom line will be that both of them can be performed in $O\left(|(\Lambda_F, T)|\,\log\left(|(\Lambda_F, T)|\right)\right)$, i.e. that up to a logarithmic factor, optimal computational complexity is achievable.

We start by outlining how the `rt` can be implemented. In order to do so, we first need to establish some auxiliary result.

**Definition 3.3.7** (Folding operations)**.** Let $n, N_x, N_y \in \mathbb{Z}^{\geq 1}$,

$$\hat{\Omega}_> = \left[-\lceil\frac{nN_x - 1}{2}\rceil : \lfloor\frac{nN_x - 1}{2}\rfloor\right] \times \left[-\lceil\frac{N_y - 1}{2}\rceil : \lfloor\frac{N_y - 1}{2}\rfloor\right]$$

$$\hat{\Omega}_< = \left[-\lceil\frac{N_x - 1}{2}\rceil : \lfloor\frac{N_x - 1}{2}\rfloor\right] \times \left[-\lceil\frac{N_y - 1}{2}\rceil : \lfloor\frac{N_y - 1}{2}\rfloor\right]$$

and $\hat{f}_> : \hat{\Omega}_> \to \mathbb{C}$. Then, $\texttt{foldx}[\hat{f}_>, n, N_x] : \hat{\Omega}_< \to \mathbb{C}$ is defined as

$$\texttt{foldx}[\hat{f}_>, n, N_x](\hat{x}, \hat{y}) := \begin{cases} \sum\limits_{\hat{v} \in \left[-\lceil\frac{n-1}{2}\rceil : \lfloor\frac{n-1}{2}\rfloor\right]} \hat{f}_>\left(\hat{x} + N_x\hat{v}, \hat{y}\right) & \hat{x} \geq 0 \\ \sum\limits_{\hat{v} \in \left[-\lfloor\frac{n-1}{2}\rfloor : \lceil\frac{n-1}{2}\rceil\right]} \hat{f}_>\left(\hat{x} + N_x\hat{v}, \hat{y}\right) & \hat{x} < 0 \end{cases}$$

and the symbol `foldx` is called the `x`-*folding operator*.

The `y`-*folding operator* `foldy` is defined likewise.

**Lemma 3.3.8** (Folding lemma)**.** *Let* $n, N_x, N_y \in \mathbb{Z}^{\geq 1}$, $L_x, L_y \in \mathbb{R}^{>0}$ *and*

$$\Omega_> = \left[0 : \frac{L_x}{nN_x} : L_x\right) \times \left[0 : \frac{L_y}{N_y} : L_y\right)$$

$$\hat{\Omega}_> = \left[-\lceil\frac{nN_x - 1}{2}\rceil : \lfloor\frac{nN_x - 1}{2}\rfloor\right] \times \left[-\lceil\frac{N_y - 1}{2}\rceil : \lfloor\frac{N_y - 1}{2}\rfloor\right]$$

$$\Omega_< = \left[0 : \frac{L_x}{N_x} : L_x\right) \times \left[0 : \frac{L_y}{N_y} : L_y\right)$$

$$\hat{\Omega}_< = \left[-\lceil\frac{N_x - 1}{2}\rceil : \lfloor\frac{N_x - 1}{2}\rfloor\right] \times \left[-\lceil\frac{N_y - 1}{2}\rceil : \lfloor\frac{N_y - 1}{2}\rfloor\right]$$

*Furthermore, let* $\hat{f}_> : \hat{\Omega}_> \to \mathbb{C}$ *and* $f_< := \texttt{ift}[\hat{f}_>]\Big|_{\Omega_<}$. *Then, we have*

$$\texttt{ft}[f_<] = \texttt{foldx}[\hat{f}_>, n, N_x]$$

*Proof.* First, assume $\hat{x} \geq 0$. Then,

$$\begin{aligned}
&\texttt{ft}[f_<](\hat{x},\hat{y}) = \dots \\
&\quad = \frac{1}{N_x N_y} \sum_{(x,y)\in\Omega_<} \texttt{ift}[\hat{f}_>](x,y)\, e^{-2\pi i\,(\hat{x}\frac{x}{L_x}+\hat{y}\frac{y}{L_y})} \\
&\quad = \frac{1}{N_x N_y} \sum_{(x,y)\in\Omega_<} \underbrace{\frac{1}{n}\left(\sum_{\hat{v}\in\left[-\lceil\frac{n-1}{2}\rceil:\lfloor\frac{n-1}{2}\rfloor\right]} e^{-2\pi i\, N_x\hat{v}\frac{x}{L_x}}\right)}_{1} \texttt{ift}[\hat{f}_>](x,y)\, e^{-2\pi i\,(\hat{x}\frac{x}{L_x}+\hat{y}\frac{y}{L_y})} + \dots \\
&\qquad \frac{1}{N_x N_y} \sum_{(x,y)\in\Omega_<} \sum_{v\in\Delta\Omega_x} \underbrace{\frac{1}{n}\left(\sum_{\hat{v}\in\left[-\lceil\frac{n-1}{2}\rceil:\lfloor\frac{n-1}{2}\rfloor\right]} e^{-2\pi i\, N_x\hat{v}\frac{x+v}{L_x}}\right)}_{0} \texttt{ift}[\hat{f}_>](x+v,y)\, e^{-2\pi i\,(\hat{x}\frac{x+v}{L_x}+\hat{y}\frac{y}{L_y})}
\end{aligned}$$

where $\Delta\Omega_x := \left(0 : \frac{L_x}{nN_x} : \frac{L_x}{N_x}\right)$. The first underbrace is 1 because $N_x\frac{x}{L_x}$ is always an integer for $x \in \Omega_<$. On the other hand, $N_x\frac{x+v}{L_x}$ for $x \in \Omega_<$ and $v \in \Delta\Omega_x$ is always a proper fraction, therefore the second underbrace collapses to zero due to the summation property of the root of unity.

Note that

$$\sum_{(x,y)\in\Omega_<} g(x,y) + \sum_{(x,y)\in\Omega_<} \sum_{v\in\Delta\Omega_x} g(x+v,y) = \sum_{(x,y)\in\Omega_>} g(x,y)$$

Therefore, we can continue the above equations with

$$\begin{aligned}
\texttt{ft}[f_<](\hat{x},\hat{y}) &= \frac{1}{n\,N_x N_y} \sum_{(x,y)\in\Omega_>} \sum_{\hat{v}\in\left[-\lceil\frac{n-1}{2}\rceil:\lfloor\frac{n-1}{2}\rfloor\right]} \texttt{ift}[\hat{f}_>](x,y)\, e^{-2\pi i\left((\hat{x}+N_x\hat{v})\frac{x}{L_x}+\hat{y}\frac{y}{L_y}\right)} \\
&= \sum_{\hat{v}\in\left[-\lceil\frac{n-1}{2}\rceil:\lfloor\frac{n-1}{2}\rfloor\right]} \frac{1}{n\,N_x N_y} \sum_{(x,y)\in\Omega_>} \texttt{ift}[\hat{f}_>](x,y)\, e^{-2\pi i\left((\hat{x}+N_x\hat{v})\frac{x}{L_x}+\hat{y}\frac{y}{L_y}\right)} \\
&= \sum_{\hat{v}\in\left[-\lceil\frac{n-1}{2}\rceil:\lfloor\frac{n-1}{2}\rfloor\right]} \texttt{ft}[\texttt{ift}[\hat{f}_>]]\,(\hat{x}+N_x\hat{v},\hat{y}) \\
&= \sum_{\hat{v}\in\left[-\lceil\frac{n-1}{2}\rceil:\lfloor\frac{n-1}{2}\rfloor\right]} \hat{f}_>\,(\hat{x}+N_x\hat{v},\hat{y}) \\
&= \texttt{foldx}[\hat{f}_>, n, N_x](\hat{x},\hat{y})
\end{aligned}$$

(remember $\hat{x} \geq 0$).

The proof for $\hat{x} < 0$ is the same except that the range of $\hat{v}$ is shifted by $+1$ if $n$ is even. Since $e^{-2\pi i(-\frac{n}{2})\frac{k}{n}} = e^{-2\pi i \frac{n}{2}\frac{k}{n}}$, the term which is dropped on the negative side in the sums over $\hat{v}$ in that case is equal to the new term on the positive side, therefore the above arguments showing that one underbrace is 1 whereas the other is 0 work out exactly the same. □

This result can now be used for evaluating the ridgelet transform for some fixed $\lambda \in \Lambda$.

**Lemma 3.3.9.** *Let $\hat{\Omega}_F$ be as in Definition 3.3.3. The complexity of evaluating*

$$\tilde{f}_\lambda(t) := \frac{1}{T_x^\lambda T_y^\lambda} \sum_{(\hat{x},\hat{y})\in\hat{\Omega}_F} \hat{f}(\hat{x},\hat{y})\,\hat{\psi}_\lambda(\hat{x},\hat{y})\,e^{2\pi i\,(\hat{x}\frac{t_x}{L_x}+\hat{y}\frac{t_y}{L_y})}$$

*for some fixed $\lambda \in \Lambda$ and all $t \in T^\lambda$ is $O\left(T_x^\lambda T_y^\lambda \log(T_x^\lambda T_y^\lambda)\right)$.*

*Proof.* We will show the lemma only for the case $\lambda = (j, \kappa = \mathtt{x}, k)$. For $\kappa \in \{\mathtt{y}, \mathtt{d}\}$, the proof is analogous and for $\kappa = \mathtt{s}$ it is trivial.

Note that the above expression corresponds to $\tilde{f}_\lambda = \frac{1}{T_x^\lambda T_y^\lambda}\mathtt{ift}[\hat{f}\hat{\psi}_\lambda]$ except that the sizes of the domains of $\tilde{f}_\lambda$ and $\hat{f}\hat{\psi}_\lambda$ (i.e. $T^\lambda$ and $\hat{\Omega}_F$) match only in $\mathtt{x}$-direction, but not necessarily in $\mathtt{y}$. Because the support of $\hat{\psi}_\lambda$ is contained within

$$\hat{\Omega}_> := \left[-\lceil\frac{T_x^\lambda - 1}{2}\rceil : \lfloor\frac{T_x^\lambda - 1}{2}\rfloor\right] \times \left[-\lceil\frac{(|k|+1)\,T_y^\lambda - 1}{2}\rceil : \lfloor\frac{(|k|+1)\,T_y^\lambda - 1}{2}\rfloor\right]$$

we can restrict the domain of $\hat{f}\hat{\psi}_\lambda$ from $\hat{\Omega}_F$ to $\hat{\Omega}_>$ such that the domain of $\mathtt{ift}[\hat{f}\hat{\psi}_\lambda]$ will be

$$\Omega_> := \left[0 : \frac{L_x}{T_x^\lambda} : L_x\right) \times \left[0 : \frac{L_y}{(|k|+1)\,T_y^\lambda} : L_y\right)$$

But we want to evaluate $\tilde{f}_\lambda$ only on

$$\Omega_< := T^\lambda = \left[0 : \frac{L_x}{T_x^\lambda} : L_x\right) \times \left[0 : \frac{L_y}{T_y^\lambda} : L_y\right)$$

thus we apply the folding lemma 3.3.8 and compute $\tilde{f}_\lambda$ as

$$\tilde{f}_\lambda(t) = \frac{1}{T_x^\lambda T_y^\lambda}\,\mathtt{ift}\left[\mathtt{foldy}\left[\hat{f}\hat{\psi}_\lambda,\, |k|+1,\, T_y^\lambda\right]\right]$$

Since the number of points in the support of $\hat{\psi}_\lambda$ is bounded by $T_x^\lambda T_y^\lambda$, we can evaluate the sums in $\mathtt{foldy}$ for all $(\hat{x},\hat{y}) \in \left[-\lceil\frac{T_x^\lambda-1}{2}\rceil : \lfloor\frac{T_x^\lambda-1}{2}\rfloor\right] \times \left[-\lceil\frac{T_y^\lambda-1}{2}\rceil : \lfloor\frac{T_y^\lambda-1}{2}\rfloor\right]$ in only $O(T_x^\lambda T_y^\lambda)$. The dominating computational effort is thus the $\mathtt{ift}$ whose complexity is known to be $O\left(T_x^\lambda T_y^\lambda \log(T_x^\lambda T_y^\lambda)\right)$ (see 2.4.6). □

The following diagram can be helpful for understanding the above arguments:

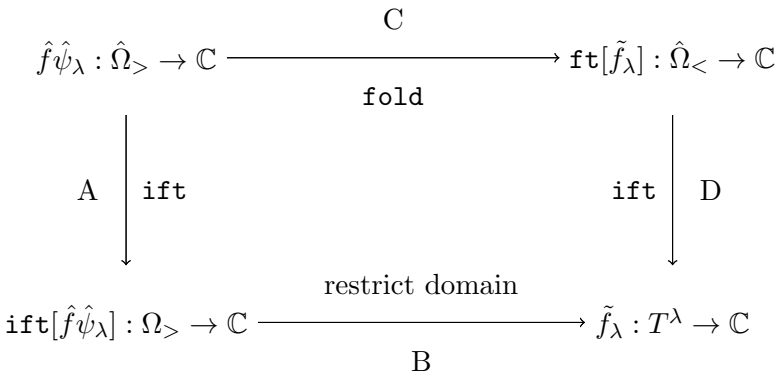


First, the folding lemma 3.3.8 establishes arrow C by going along A, B and the inverse of D. Then, Lemma 3.3.9 proves that the overall complexity of going along arrows C and D is $O\left(T_x^\lambda T_y^\lambda \log(T_x^\lambda T_y^\lambda)\right)$. Note that this is less than going along A and B since in step A we would destroy the sparsity structure of supp $\hat{f}\hat{\psi}_\lambda$.

With the work done so far, proving the overall complexity of the `rt` becomes easy.

**Theorem 3.3.10** (Complexity of `rt`)**.** *Let $J_{min} = \min\{J_x, J_y\}$ and $J_{max} = \max\{J_x, J_y\}$. Then, the complexity of evaluating* `rt` *for all $\lambda \in \Lambda_F$ and $t \in T^\lambda$ is*

$$O\left(\log(\rho_x\rho_y)\,\rho_x\rho_y\left(J_{min}\,4^{J_{min}} + J_{max}\,2^{J_{max}}\right)\right)$$

*Proof.* By lemma 3.3.9 and the definition of the translation sets $T^\lambda$ 3.1.10 we know that the complexity of evaluating $\texttt{rt}[\hat{f}](\lambda, t)$ for some fixed $\lambda \in \Lambda$ and all $t \in T^\lambda$ is $O\left(\log(\rho_x\rho_y)\,\rho_x\rho_y\,j\,2^j\right)$. On a fixed scale $j$ we have $O(2^{\min\{j, J_{min}\}})$ ridgelets, and thus the overall complexity is

$$\begin{aligned}\sum_{j=0}^{J_{min}} O\left(2^j\right)\, O\left(\log(\rho_x\rho_y)\,\rho_x\rho_y\,j\,2^j\right) + \sum_{j=J_{min}+1}^{J_{max}} O\left(2^{J_{min}}\right)\, O\left((\log(\rho_x\rho_y)\,\rho_x\rho_y\,j\,2^j\right) \\ = O\left(\log(\rho_x\rho_y)\,\rho_x\rho_y\left(J_{min}\,4^{J_{min}} + J_{max}\,2^{J_{max}}\right)\right)\end{aligned}$$

□

The algorithm for evaluating the `irt` is derived in exactly the same way.

**Definition 3.3.11** (Unfolding operations)**.** Let $n, N_x, N_y \in \mathbb{Z}^{\geq 1}$,

$$\hat{\Omega}_> = \left[-\lceil\frac{nN_x - 1}{2}\rceil : \lfloor\frac{nN_x - 1}{2}\rfloor\right] \times \left[-\lceil\frac{N_y - 1}{2}\rceil : \lfloor\frac{N_y - 1}{2}\rfloor\right]$$

$$\hat{\Omega}_< = \left[-\lceil\frac{N_x - 1}{2}\rceil : \lfloor\frac{N_x - 1}{2}\rfloor\right] \times \left[-\lceil\frac{N_y - 1}{2}\rceil : \lfloor\frac{N_y - 1}{2}\rfloor\right]$$

and $\hat{f}_< : \hat{\Omega}_< \to \mathbb{C}$. Then, $\texttt{unfoldx}[\hat{f}_<, n, N_x] : \hat{\Omega}_> \to \mathbb{C}$ is defined as

$$\texttt{unfoldx}[\hat{f}_<, n, N_x](\hat{x}, \hat{y}) := \frac{1}{n} f_< \left( \hat{x} - N_x \, [\frac{\hat{x}}{N_x}], \, \hat{y} \right)$$

($[\cdot]$ denotes rounding to nearest integer or $+\infty$ if the nearest integer is not unique) and the symbol $\texttt{unfoldx}$ is called the $\texttt{x}$-*unfolding operator*.

The $\texttt{y}$-*unfolding operator* $\texttt{unfoldy}$ is defined likewise.

**Lemma 3.3.12** (Unfolding lemma)**.** *Let* $n, N_x, N_y \in \mathbb{Z}^{\geq 1}$, $L_x, L_y \in \mathbb{R}^{>0}$,

$$\Omega_> = \left[ 0 : \frac{L_x}{nN_x} : L_x \right) \times \left[ 0 : \frac{L_y}{N_y} : L_y \right)$$

$$\hat{\Omega}_> = \left[ -\lceil \frac{nN_x - 1}{2} \rceil : \lfloor \frac{nN_x - 1}{2} \rfloor \right] \times \left[ -\lceil \frac{N_y - 1}{2} \rceil : \lfloor \frac{N_y - 1}{2} \rfloor \right]$$

$$\Omega_< = \left[ 0 : \frac{L_x}{N_x} : L_x \right) \times \left[ 0 : \frac{L_y}{N_y} : L_y \right)$$

$$\hat{\Omega}_< = \left[ -\lceil \frac{N_x - 1}{2} \rceil : \lfloor \frac{N_x - 1}{2} \rfloor \right] \times \left[ -\lceil \frac{N_y - 1}{2} \rceil : \lfloor \frac{N_y - 1}{2} \rfloor \right]$$

*and* $\hat{f}_< : \hat{\Omega}_< \to \mathbb{C}$. *Furthermore, let* $f_> : \Omega_> \to \mathbb{C}$ *be given by*

$$f_>(x, y) := \begin{cases} \texttt{ift}[\hat{f}_<](x, y) & \text{if } (x, y) \in \Omega_< \\ 0 & \text{otherwise} \end{cases}$$

*Then, we have*

$$\texttt{ft}[f_>] = \texttt{unfoldx}[\hat{f}_<, n, N_x]$$

*Proof.*

$$\begin{aligned} \texttt{ft}[f_>](\hat{x}, \hat{y}) &= \frac{1}{n \, N_x N_y} \sum_{(x,y) \in \Omega_>} f_>(x, y) \, e^{-2\pi i \, (\hat{x} \frac{x}{L_x} + \hat{y} \frac{y}{L_y})} \\ &= \frac{1}{n \, N_x N_y} \sum_{(x,y) \in \Omega_<} \texttt{ift}[\hat{f}_<](x, y) \, e^{-2\pi i \, (\hat{x} \frac{x}{L_x} + \hat{y} \frac{y}{L_y})} \\ &= \frac{1}{n} \frac{1}{N_x N_y} \sum_{(x,y) \in \Omega_<} \texttt{ift}[\hat{f}_<](x, y) \, e^{-2\pi i \left( \left( \hat{x} - N_x [\frac{\hat{x}}{N_x}] \right) \frac{x}{L_x} + \hat{y} \frac{y}{L_y} \right)} \end{aligned}$$

(The additional term in the exponential can be added because $N_x \frac{x}{L_x}$ is always an integer.)

$$\begin{aligned} &= \frac{1}{n} \, \texttt{ft}[\texttt{ift}[\hat{f}_<]] \left( \hat{x} - N_x [\frac{\hat{x}}{N_x}], \, \hat{y} \right) \\ &= \frac{1}{n} \, \hat{f}_< \left( \hat{x} - N_x [\frac{\hat{x}}{N_x}], \, \hat{y} \right) \\ &= \texttt{unfoldx}[\hat{f}_<, n, N_x](\hat{x}, \, \hat{y}) \end{aligned}$$

□

**Lemma 3.3.13.** *The complexity of evaluating*

$$\hat{f}_\lambda(\hat{x},\hat{y}) := \sum_{t\in T^\lambda} \tilde{f}(\lambda,t)\, e^{-2\pi i\,(\hat{x}\frac{t_x}{L_x}+\hat{y}\frac{t_y}{L_y})}$$

*for some fixed* $\lambda\in\Lambda$ *and all* $(\hat{x},\hat{y})\in\operatorname{supp}\hat{\psi}_\lambda$ *is* $O\left(T_x^\lambda T_y^\lambda \log(T_x^\lambda T_y^\lambda)\right)$.

*Proof.* We will show the lemma only for the case $\lambda=(j,\kappa=\mathtt{x},k)$. For $\kappa\in\{\mathtt{y},\mathtt{d}\}$, the proof is analogous and for $\kappa=\mathtt{s}$ it is trivial.

Note that the above expression corresponds to $\hat{f}_\lambda = T_x^\lambda T_y^\lambda\,\mathtt{ft}[\tilde{f}(\lambda,\cdot)]$ except that we want the domain of $\mathtt{ft}[\tilde{f}(\lambda,\cdot)]$ to be not

$$\hat{\Omega}_< := \left[-\lceil\frac{T_x^\lambda-1}{2}\rceil : \lfloor\frac{T_x^\lambda-1}{2}\rfloor\right]\times\left[-\lceil\frac{T_y^\lambda-1}{2}\rceil : \lfloor\frac{T_y^\lambda-1}{2}\rfloor\right]$$

but rather a subset of

$$\hat{\Omega}_> := \left[-\lceil\frac{T_x^\lambda-1}{2}\rceil : \lfloor\frac{T_x^\lambda-1}{2}\rfloor\right]\times\left[-\lceil\frac{(|k|+1)\,T_y^\lambda-1}{2}\rceil : \lfloor\frac{(|k|+1)\,T_y^\lambda-1}{2}\rfloor\right]$$

We can achieve this by defining

$$T_>^\lambda := \left[0 : \frac{L_x}{T_x^\lambda} : L_x\right)\times\left[0 : \frac{L_y}{(|k|+1)\,T_y^\lambda} : L_y\right)$$

$$\tilde{f}_>(\lambda,\cdot) : T_>^\lambda\to\mathbb{C},\ t\mapsto\begin{cases}\tilde{f}(\lambda,t) & \text{if } t\in T^\lambda\\ 0 & \text{otherwise}\end{cases}$$

Because all new terms in the $\mathtt{ft}$ sum are zero, writing $\hat{f}_\lambda = T_x^\lambda\,(|k|+1)\,T_y^\lambda\,\mathtt{ft}[\tilde{f}_>(\lambda,\cdot)]$ is now correct both in terms of equal values as well as equal domains. Running the $\mathtt{ft}$ on a function which is mostly zero seems to be a waste of effort, however, and indeed the unfolding lemma 3.3.12 shows that the above expression is equivalent to

$$\hat{f}_\lambda(\hat{x},\hat{y}) = T_x^\lambda\,(|k|+1)\,T_y^\lambda\,\mathtt{unfoldy}\Big[\mathtt{ft}[\tilde{f}(\lambda,\cdot)],\,|k|+1,\,T_y^\lambda\Big]\,(\hat{x},\hat{y})$$

We evaluate the $\mathtt{unfoldy}$ only on $O(T_x^\lambda T_y^\lambda)$ points, and each point evaluation can be done in $O(1)$ once $\mathtt{ft}[\tilde{f}(\lambda,\cdot)]$ is available. The dominating computational effort is thus computing the $\mathtt{ft}$ which can be done in $O\left(T_x^\lambda T_y^\lambda\log(T_x^\lambda T_y^\lambda)\right)$, see Theorem 2.4.6. □

Again, it is helpful to visualize what is happening in a diagram:

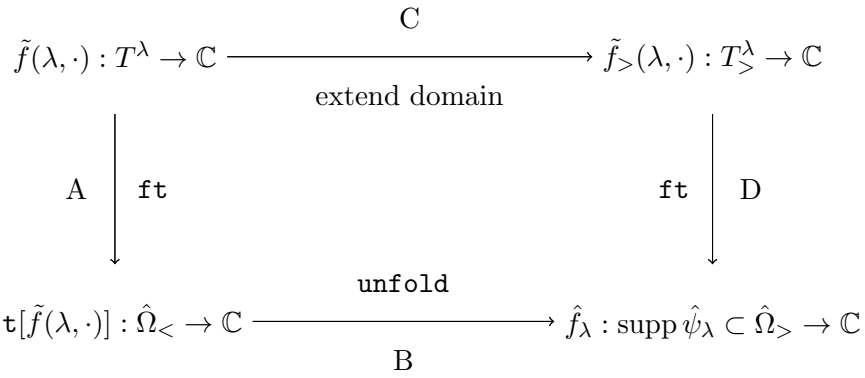


The unfolding lemma 3.3.12 establishes arrow B by going along the inverse of A and C, D. Then, Lemma 3.3.13 proves that the overall complexity of going along arrows A and B is $O\left(T_x^\lambda T_y^\lambda \log(T_x^\lambda T_y^\lambda)\right)$. Note that this is less than going along C and D since in step D we would have to compute the `ft` of the extended $\tilde{f}_>(\lambda,\cdot)$.

As before, the overall complexity of the `irt` simply follows from the above lemma.

**Theorem 3.3.14** (Complexity of `irt`)**.** *Let* $J_{min} = \min\{J_x, J_y\}$ *and* $J_{max} = \max\{J_x, J_y\}$. *Then, the complexity of evaluating* `irt` *for all* $(\hat{x}, \hat{y})$ *in its domain is*

$$O\left(\log(\rho_x\rho_y)\,\rho_x\rho_y\left(J_{min}\,4^{J_{min}} + J_{max}\,2^{J_{max}}\right)\right)$$

*Proof.* The only thing which is different from the proof of the complexity of `rt` in 3.3.10 is that in the end we have to sum up all the $\hat{f}_\lambda$. Since every point in the Fourier space lies in the support of at most four ridgelets and we evaluate the `irt` on $O\left(\rho_x\rho_y(4^{J_{min}} + 2^{J_{max}})\right)$ points, that sum does not dominate the overall complexity. □

We have seen that the finite ridgelet transforms can in theory achieve an almost optimal computational complexity of $O(N\log(N))$ where $N$ is (proportional to) the number of input and output parameters. Achieving the same complexity in a practical implementation requires a lot of work, however, since the `fold` and `unfold` methods need to be able to exploit the special sparsity structures exhibited by the supports of the ridgelets [5]. The Matlab implementation which comes with this bachelor thesis achieves only a theoretical scaling of $O(N^{\frac{3}{2}})$ but therefore uses fast Matlab built-in algorithms for folding and unfolding. Figure 3.2 shows that like this, the $O(N^{\frac{3}{2}})$ scaling can only be observed for very large $N$ where the algorithms reach their compute power and memory limits anyway.

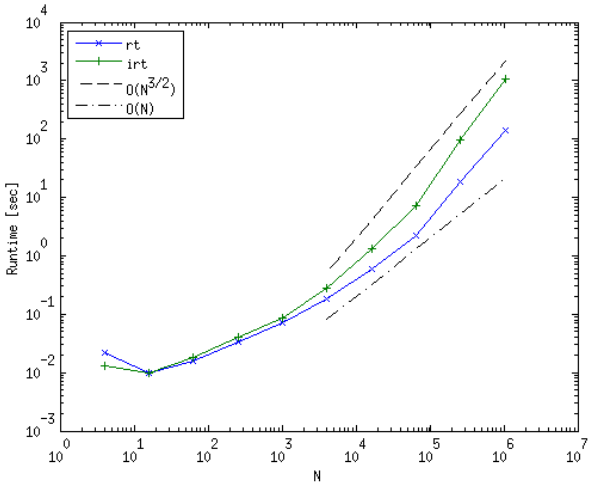


Figure 3.2: Scaling plot of `rt` and `irt`. $\rho_x = \rho_y = 1$ and $J_x = J_y \in [1 : 10]$ were used. $N$ was computed as $4^J$.

# 4 Intermezzo: Scalar Products

The aim of the previous chapters on Fourier theory and ridgelets is to develop solvers for the radiative transport equation. Before we can tackle that task, we first have to put one more piece into place, however: We need to choose scalar products for the different function spaces, and we need to show some relations between these scalar products.

## 4.1 Definitions

**Definition 4.1.1** (Finite real space scalar product)**.** Let $N_x, N_y$ and $\Omega_F$ be as in the definition of the finite Fourier transform 2.4.1 and $f, g : \Omega_F \to \mathbb{C}$. Then, the finite real space scalar product of $f$ and $g$ is given by

$$\langle f, g \rangle_{\Omega_F} := \frac{1}{N_x N_y} \sum_{(x,y) \in \Omega_F} f(x,y)\, \overline{g(x,y)}$$

**Definition 4.1.2** (Finite Fourier space scalar product)**.** Let $\hat{\Omega}_F$ be as in the definition of the finite Fourier transform 2.4.1 and $\hat{f}, \hat{g} : \hat{\Omega}_F \to \mathbb{C}$. Then, the finite Fourier space scalar product of $\hat{f}$ and $\hat{g}$ is given by

$$\langle \hat{f}, \hat{g} \rangle_{\hat{\Omega}_F} := \sum_{(\hat{x},\hat{y}) \in \hat{\Omega}_F} \hat{f}(\hat{x},\hat{y})\, \overline{\hat{g}(\hat{x},\hat{y})}$$

**Definition 4.1.3** (Finite ridgelet coefficient space scalar product)**.** Let $\tilde{f}, \tilde{g} : (\Lambda_F, T) \to \mathbb{C}$. Then, the finite ridgelet coefficient space scalar product of $\tilde{f}$ and $\tilde{g}$ is given by

$$\langle \tilde{f}, \tilde{g} \rangle_{(\Lambda_F,T)} := \sum_{\lambda \in \Lambda_F} T_x^\lambda T_y^\lambda \sum_{t \in T^\lambda} \tilde{f}(\lambda,t)\, \overline{\tilde{g}(\lambda,t)}$$

## 4.2 Relations

The above scalar products correspond to the standard $\ell^2$ scalar product with some additional prefactors. The purpose of these prefactors is to assert that the scalar products are preserved under the Fourier and ridgelet transforms.

**Theorem 4.2.1** (Real/Fourier space scalar product equivalence)**.** *Let $\Omega_F$ be as in the definition of the finite Fourier transform 2.4.1 and $f, g : \Omega_F \to \mathbb{C}$. Then, we have*

$$\langle f, g \rangle_{\Omega_F} = \langle \mathtt{ft}[f], \mathtt{ft}[g] \rangle_{\hat{\Omega}_F}$$

*Proof.* Note that the above equation is the finite analogue to the Plancherel formula 2.3.6. The proof is exactly the same as in the continuous case, except that the infinite spaces are replaced with their finite counterparts and the series and integrals are replaced by sums. □

**Theorem 4.2.2** (Fourier/ridgelet space scalar product equivalence)**.** *Let $\hat{\Omega}_F$ be as in the definition of the finite Fourier transform 2.4.1, $\hat{f} : \hat{\Omega}_F \to \mathbb{C}$ and $\tilde{g} : (\Lambda_F, T) \to \mathbb{C}$. Then, we have*

$$\langle \hat{f}, \mathtt{irt}[\tilde{g}] \rangle_{\hat{\Omega}_F} = \langle \mathtt{rt}[\hat{f}], \tilde{g} \rangle_{(\Lambda_F, T)}$$

*Proof.*

$$\begin{aligned}
\langle \hat{f},\, \mathtt{irt}[\tilde{g}] \rangle_{\hat{\Omega}_F} &= \sum_{(\hat{x},\hat{y}) \in \hat{\Omega}_F} \hat{f}(\hat{x},\hat{y}) \overline{\sum_{\lambda \in \Lambda_F} \sum_{t \in T^\lambda} \tilde{g}(\lambda, t)\, \hat{\psi}_\lambda(\hat{x},\hat{y})\, e^{-2\pi i \left(\hat{x}\frac{t_x}{L_x} + \hat{y}\frac{t_y}{L_y}\right)}} \\
&= \sum_{\lambda \in \Lambda_F} T_x^\lambda T_y^\lambda \sum_{t \in T^\lambda} \left( \frac{1}{T_x^\lambda T_y^\lambda} \sum_{(\hat{x},\hat{y}) \in \hat{\Omega}_F} \hat{f}(\hat{x},\hat{y}) \hat{\psi}_\lambda(\hat{x},\hat{y})\, e^{2\pi i \left(\hat{x}\frac{t_x}{L_x} + \hat{y}\frac{t_y}{L_y}\right)} \right) \overline{\tilde{g}(\lambda, t)} \\
&= \langle \mathtt{rt}[\hat{f}],\, \tilde{g} \rangle_{(\Lambda_F, T)}
\end{aligned}$$

□

Because the finite Fourier transforms are mutually inverse, we can substitute $f$ with $\mathtt{ift}[\hat{f}]$ or $g$ with $\mathtt{ift}[\hat{g}]$ and get all the following equivalences for free:

$$\langle f, \mathtt{ift}[\hat{g}] \rangle_{\Omega_F} = \langle \mathtt{ft}[f], \hat{g} \rangle_{\hat{\Omega}_F}$$

$$\langle \mathtt{ift}[\hat{f}], g \rangle_{\Omega_F} = \langle \hat{f}, \mathtt{ft}[g] \rangle_{\hat{\Omega}_F}$$

$$\langle \mathtt{ift}[\hat{f}], \mathtt{ift}[\hat{g}] \rangle_{\Omega_F} = \langle \hat{f}, \hat{g} \rangle_{\hat{\Omega}_F}$$

It is important to stress that the same is *not* true for the ridgelet transforms, however! In fact,

$$\langle \mathtt{irt}[\tilde{f}], \hat{g} \rangle_{\hat{\Omega}_F} = \langle \tilde{f}, \mathtt{rt}[\hat{g}] \rangle_{(\Lambda_F, T)}$$

is the only correct additional equivalence to the one shown in Theorem 4.2.2, and the right argument to prove its correctness is the conjugate symmetry of the scalar products.

Since $\hat{\mathcal{R}}^{-1} \circ \hat{\mathcal{R}} = \mathbb{I}$, one might think that

$$\langle \hat{f}, \hat{g} \rangle_{\hat{\Omega}_F} \neq \langle \mathtt{rt}[\hat{f}], \mathtt{rt}[\hat{g}] \rangle_{(\Lambda_F, T)} \tag{4.2.1}$$

should be an equality as it seems that we can substitute $\tilde{g}$ with $\mathtt{rt}[\hat{g}]$ in Theorem 4.2.2. But remember from Section 3.3 that $\mathtt{irt} \circ \mathtt{rt}$ holds only on the region where the frame constitutes a partition of unity, which in this case is not the entire domain of $\hat{g}$. For example, if we have a square frame with $J_x = J_y = J$, $\rho_x = \rho_y = \rho$ and choose

$$\hat{g}(\hat{x},\hat{y}) = \delta\left(\hat{x} + \rho 2^{J+1}\right) + \delta\left(\hat{y} + \rho 2^{J+1}\right)$$

we have that $\texttt{irt}[\texttt{rt}[\hat{g}]](\hat{x},\hat{y}) = 0$ for all $(\hat{x},\hat{y})$ because no ridgelet covers that highest frequency part. With that $\hat{g}$, the right hand side in (4.2) is zero for all $\hat{f}$ while the left hand side is not.

Finally,

$$\langle \texttt{irt}[\tilde{f}], \texttt{irt}[\tilde{g}] \rangle_{\hat{\Omega}_F} \neq \langle \tilde{f}, \tilde{g} \rangle_{(\Lambda_F, T)}$$

would not even become an equality for the infinite ridgelet transforms, because due to the redundancy in ridgelet coefficient space the inverse ridgelet transforms must have a kernel $K$. If we thus choose e.g. $\tilde{f}, \tilde{g} \in K$, then the left hand side is zero while the right hand side is not necessarily.

# 5 Radiative Transport Equation

## 5.1 Basic RTE Solver

In order to get started, let us consider the following simplified version of the radiative transport equation

$$s \cdot \nabla u + \kappa\, u = f \tag{5.1.1}$$

where here $u, \kappa, f : \Omega \to \mathbb{R}$, i.e. we neglect scattering and consider only a fixed direction $s \in \mathbb{S}^1$ (we set again $\Omega := [0, L_x) \times [0, L_y)$ and $\mathbb{S}^1 := \{s \in \mathbb{R}^2 \mid \|s\|_2 = 1\}$). In the following, we will write the solution $u$ as the inverse Fourier transform $\mathcal{F}^{-1}[\hat{u}]$ of some Fourier space function $\hat{u}$. A necessary consequence of this approach is that we must consider periodic boundary conditions

$$u(0, y) = u(L_x, y), \quad u(x, 0) = u(x, L_y) \quad \forall x \in [0, L_x) \text{ and } y \in [0, L_y)$$

(remember the discussion on the inherent periodicity of the Fourier transforms after definition 2.3.2). Although such boundary conditions are rarely physically justified, they do not prevent us from solving real-world problems either. For example, if we want to simulate zero inflow boundary conditions, we can enlarge the domain or artificially increase $\kappa$ near the boundary such that all the radiation is absorbed within one period. General Dirichlet boundary conditions can be imposed through a clever choice of $\kappa$ and $f$ near the boundary, see Section 6.3.

In this simplified case considered here, it is easy to discretize the RTE:

**Definition 5.1.1** (Fourier space RTE operator)**.** Let $L_x, L_y \in \mathbb{Z}^{>0}$, $s \in \mathbb{S}^1$, $\kappa : [0, L_x) \times [0, L_y) \to \mathbb{R}$ and $\hat{f} : \mathbb{Z}^2 \to \mathbb{C}$. Then, $\hat{\mathcal{T}}[\hat{f}] : \mathbb{Z}^2 \to \mathbb{C}$ is a function given by

$$\hat{\mathcal{T}}[\hat{f}](\hat{x}, \hat{y}) := 2\pi i\, s \cdot \left(\frac{\hat{x}}{L_x}, \frac{\hat{y}}{L_y}\right)^T \hat{f}(\hat{x}, \hat{y}) + \mathcal{F}\left[\kappa\, \mathcal{F}^{-1}[\hat{f}]\right](\hat{x}, \hat{y})$$

and the symbol $\hat{\mathcal{T}}$ is called the *Fourier space RTE operator*.

**Definition 5.1.2** (Ridgelet coefficient space RTE operator)**.** Let $\tilde{f} : (\Lambda, T) \to \mathbb{C}$. Then, $\tilde{\mathcal{T}}[\tilde{f}](\lambda, t) : (\Lambda, T) \to \mathbb{C}$ is a function given by

$$\tilde{\mathcal{T}}[\tilde{f}](\lambda, t) := \hat{\mathcal{R}}\left[\hat{\mathcal{T}}\left[\hat{\mathcal{R}}^{-1}[\tilde{f}]\right]\right](\lambda, t)$$

and the symbol $\tilde{\mathcal{T}}$ is called the *ridgelet coefficient space RTE operator*.

It can easily be verified that

$$s \cdot \nabla u + \kappa\, u = f \iff \hat{\mathcal{T}}[\mathcal{F}[u]] = \mathcal{F}[f] \iff \tilde{\mathcal{T}}[\mathcal{R}[u]] = \mathcal{R}[f]$$

Since both $\mathcal{F}$ and $\mathcal{R}$ have left inverses, we can thus solve (5.1) by solving either of

$$\hat{\mathcal{T}}[\hat{u}] = \mathcal{F}[f], \quad u = \mathcal{F}^{-1}[\hat{u}] \tag{5.1.2}$$

$$\tilde{\mathcal{T}}[\tilde{u}] = \mathcal{R}[f], \quad u = \mathcal{R}^{-1}[\tilde{u}] \tag{5.1.3}$$

Neither of these problems can yet be solved numerically as they involve infinitely many equations in infinitely many unknowns. But with the finite transforms developed in Chapter 2 and 3, the following approximations come naturally.

**Definition 5.1.3** (Finite Fourier space RTE operator)**.** Let $L_x, L_y \in \mathbb{Z}^{>0}$, $s \in \mathbb{S}^1$, $N_x, N_y \in \mathbb{Z}^{\geq 1}$,

$$\Omega_F = \left[0 : \frac{L_x}{N_x} : L_x\right) \times \left[0 : \frac{L_y}{N_y} : L_y\right)$$

$$\hat{\Omega}_F = \left[-\lceil \frac{N_x - 1}{2} \rceil : \lfloor \frac{N_x - 1}{2} \rfloor\right] \times \left[-\lceil \frac{N_y - 1}{2} \rceil : \lfloor \frac{N_y - 1}{2} \rfloor\right]$$

$\kappa : \Omega_F \to \mathbb{R}$ and $\hat{f} : \hat{\Omega}_F \to \mathbb{C}$. Then, $\texttt{Tfs}[\hat{f}] : \hat{\Omega}_F \to \mathbb{C}$ is a function given by

$$\texttt{Tfs}[\hat{f}](\hat{x}, \hat{y}) := 2\pi i\, s \cdot \left(\frac{\hat{x}}{L_x}, \frac{\hat{y}}{L_y}\right)^T \hat{f}(\hat{x}, \hat{y}) + \texttt{ft}\left[\kappa\, \texttt{ift}[\hat{f}]\right](\hat{x}, \hat{y})$$

and the symbol `Tfs` is called the *finite Fourier space RTE operator*.

**Definition 5.1.4** (Finite ridgelet coefficient space RTE operator)**.** Let $\tilde{f} : (\Lambda_F, T) \to \mathbb{C}$. Then, $\texttt{Trcs}[\tilde{f}] : (\Lambda_F, T) \to \mathbb{C}$ is a function given by

$$\texttt{Trcs}[\tilde{f}](\lambda, t) := \texttt{rt}\left[\texttt{Tfs}\left[\texttt{irt}[\tilde{f}]\right]\right](\lambda, t)$$

and the symbol `Trcs` is called the *finite ridgelet coefficient space RTE operator*.

With these new operators, (5.1) and (5.1) become

$$\texttt{Tfs}[\hat{u}] = \texttt{ft}[f], \quad u = \texttt{ift}[\hat{u}] \tag{5.1.4}$$

$$\texttt{Trcs}[\tilde{u}] = \texttt{rt}\left[\texttt{ft}[f]\right], \quad u = \texttt{ift}\left[\texttt{irt}[\tilde{u}]\right] \tag{5.1.5}$$

where here $u$ and $f$ mean the $u$ and $f$ from (5.1) sampled on the grid defined by the `(i)ft`. While it is clear that these equations correspond to linear systems of equations, formulating these systems explicitly can nevertheless be tedious. Luckily, though, it is neither necessary nor advisable. Rather, we can use iterative methods like the *conjugate gradient* (CG) iterations which have the benefit that they are able to deal with vectors in an abstract sense, i.e. vectors which only satisfy the vector axioms but are not necessarily taken from $\mathbb{R}^n$, and abstract linear operators acting on such vectors.

In this abstract formulation, problems (5.1) and (5.1) read

$$\mathcal{L}[u] = f \tag{5.1.6}$$

where $u$ and $f$ are taken from some vector space $V$ and $\mathcal{L} : V \to V$ is a linear operator. For the CG method to work, $\mathcal{L}$ has to be self-adjoint and positive (semi-)definite in the chosen norm, i.e. $\langle f, \mathcal{L}[g]\rangle = \langle \mathcal{L}[f], g\rangle$ and $\langle f, \mathcal{L}[f]\rangle \geq 0$ have to hold. If $\mathcal{L}$ does not yet satisfy these conditions, the standard approach is to solve the normal equations

$$\mathcal{L}^* \left[\mathcal{L}[u]\right] = \mathcal{L}^*[f]$$

instead of (5.1), where $\mathcal{L}^*$ denotes the adjoint of $\mathcal{L}$. Because neither `Tfs` nor `Trcs` satisfy yet the "self-adjoint and positive semidefinite" criterion, we will use CG on the normal equations as well. Therefore, we need the following two theorems.

**Theorem 5.1.5** (Adjoint of `Tfs`)**.** *The adjoint* $\texttt{Tfs}^*$ *of* `Tfs` *in the finite Fourier space scalar product is given by*

$$\texttt{Tfs}^*[\hat{f}](\hat{x}, \hat{y}) := -2\pi i\, s \cdot \left(\frac{\hat{x}}{L_x}, \frac{\hat{y}}{L_y}\right)^T \hat{f}(\hat{x}, \hat{y}) + \texttt{ft}\left[\bar{\kappa}\, \texttt{ift}[\hat{f}]\right](\hat{x}, \hat{y})$$

*Proof.* Because $(\mathcal{L} + \mathcal{K})^* = \mathcal{L}^* + \mathcal{K}^*$ for two linear operators $\mathcal{L}, \mathcal{K}$, we can show for each term in $\texttt{Tfs}^*$ separately that it is the adjoint of the respective term in `Tfs`. For the first term, this relationship is obvious. For the second, with $\hat{f}, \hat{g} : \hat{\Omega}_F \to \mathbb{C}$, we get

$$\begin{aligned}
\langle \hat{f}, \texttt{ft}\left[\kappa\, \texttt{ift}[\hat{g}]\right]\rangle_{\hat{\Omega}_F} &= \langle \texttt{ift}[\hat{f}], \kappa\, \texttt{ift}[\hat{g}]\rangle_{\Omega_F} \\
&= \langle \bar{\kappa}\, \texttt{ift}[\hat{f}], \texttt{ift}[\hat{g}]\rangle_{\Omega_F} \\
&= \langle \texttt{ft}\left[\bar{\kappa}\, \texttt{ift}[\hat{f}]\right], \hat{g}\rangle_{\hat{\Omega}_F}
\end{aligned}$$

where we have made use of the equivalence of the real and Fourier space scalar products, see Theorem 4.2.1. □

**Theorem 5.1.6** (Adjoint of `Trcs`)**.** *The adjoint* $\texttt{Trcs}^*$ *of* `Trcs` *in the finite ridgelet coefficient space scalar product is given by*

$$\texttt{Trcs}^*[\tilde{f}](\lambda, t) := \texttt{rt}\left[\texttt{Tfs}^*\left[\texttt{irt}[\tilde{f}]\right]\right](\lambda, t)$$

*Proof.* Let $\tilde{f}, \tilde{g} : (\Lambda_F, T) \to \mathbb{C}$, Then,

$$\begin{aligned}
\langle \tilde{f}, \texttt{rt}\left[\texttt{Tfs}\left[\texttt{irt}[\tilde{g}]\right]\right]\rangle_{(\Lambda_F, T)} &= \langle \texttt{irt}[\tilde{f}], \texttt{Tfs}\left[\texttt{irt}[\tilde{g}]\right]\rangle_{\hat{\Omega}_F} \\
&= \langle \texttt{Tfs}^*\left[\texttt{irt}[\tilde{f}]\right], \texttt{irt}[\tilde{g}]\rangle_{\hat{\Omega}_F} \\
&= \langle \texttt{rt}\left[\texttt{Tfs}^*\left[\texttt{irt}[\tilde{f}]\right]\right], \tilde{g}\rangle_{(\Lambda_F, T)}
\end{aligned}$$

where we used the equivalence of the Fourier and ridgelet coefficient space scalar product, see Theorem 4.2.2. □

Our equations thus become

$$\mathtt{Tfs}^* \left[\mathtt{Tfs}[\hat{u}]\right] = \mathtt{Tfs}^* \left[\mathtt{ft}[f]\right], \quad u = \mathtt{ift}[\hat{u}]$$

$$\mathtt{Trcs}^* \left[\mathtt{Trcs}[\tilde{u}]\right] = \mathtt{rt}\left[\mathtt{Tfs}^* \left[\mathtt{ft}[f]\right]\right], \quad u = \mathtt{ift}\left[\mathtt{irt}[\tilde{u}]\right]$$

and can now in theory be solved by CG. However, it is not hard to see that the directional derivative term in `Tfs` leads to very ill conditioned operators. Therefore one needs to apply preconditioners to these problems such that the final equations read

$$\left(\mathtt{D}_{\mathtt{Tfs}} \circ \mathtt{Tfs}^* \circ \mathtt{Tfs} \circ \mathtt{D}_{\mathtt{Tfs}}\right)[\hat{u}_p] = \left(\mathtt{D}_{\mathtt{Tfs}} \circ \mathtt{Tfs}^*\right)\left[\mathtt{ft}[f]\right], \quad u = \mathtt{ift}\left[\mathtt{D}_{\mathtt{Tfs}}[\hat{u}_p]\right] \tag{5.1.7}$$

$$\begin{gathered}\left(\mathtt{D}_{\mathtt{Trcs}} \circ \mathtt{Trcs}^* \circ \mathtt{Trcs} \circ \mathtt{D}_{\mathtt{Trcs}}\right)[\tilde{u}_p] = \left(\mathtt{D}_{\mathtt{Trcs}} \circ \mathtt{Trcs}^*\right)\left[\mathtt{rt}\left[\mathtt{ft}[f]\right]\right], \\ u = \mathtt{ift}\left[\mathtt{irt}\left[\mathtt{D}_{\mathtt{Trcs}}\tilde{u}_p\right]\right]\end{gathered} \tag{5.1.8}$$

with

$$\mathtt{D}_{\mathtt{Tfs}}[\hat{f}](\hat{x}, \hat{y}) := \frac{\hat{f}(\hat{x}, \hat{y})}{1 + |s_x\,\hat{x} + s_y\,\hat{y}|} \tag{5.1.9}$$

$$\mathtt{D}_{\mathtt{Trcs}}[\tilde{f}](\lambda, t) := \frac{\tilde{f}(\lambda, t)}{1 + 2^j\,|s \cdot s_\lambda|} \tag{5.1.10}$$

where $s$ is the transport direction in the RTE and

$$s_\lambda = \frac{\tilde{s}_\lambda}{\|\tilde{s}_\lambda\|_2}, \quad \tilde{s}_\lambda = \begin{cases} (0,0)^T & \text{if } \kappa = \mathtt{s} \\ (1, \frac{k}{2^{j-1}})^T & \text{if } \kappa = \mathtt{x} \\ (\frac{k}{2^{j-1}}, 1)^T & \text{if } \kappa = \mathtt{y} \\ (1,k)^T & \text{if } \kappa = \mathtt{d} \end{cases}$$

is the direction of the ridgelet $\hat{\psi}_\lambda$ in Fourier space. The ridgelet preconditioner $\mathtt{D}_{\mathtt{Trcs}}$ is based on a recent result by Grohs [1], where it is shown that this choice leads to bounded condition numbers.

## 5.2 Convergence Of Basic RTE Solver

The key step in developing the basic RTE solvers was to replace the infinite Fourier and ridgelet transforms in the RTE with their finite counterparts. Obviously, we thus bought computational feasibility at the expense of exactness of the solution. While the algorithmic complexities of the basic RTE solvers follow straightforwardly from the ones shown for the various transforms, it remains yet to analyze how large the loss in precision is. In the following, we will tackle exactly this task.

Let $u$ denote the exact solution of (5.1) and $u'$ the approximation obtained from (5.1) or (5.1), with $\hat{u}$ and $\hat{u}'$ their respective Fourier transforms. Strictly speaking, the approximate solution $u' = \mathtt{ift}[\hat{u}']$ is only defined on a discrete set of points, whereas

$u$ is defined on $\Omega := [0, L_x) \times [0, L_y)$. In order to make the two domains equal, let us extend $u'$ to a solution on $\Omega$ by writing $u' = \mathcal{F}^{-1}[\mathcal{Z}[\hat{u}']]$ (see also the discussion after the definition of the `ift` in 2.4.2). Also, let $u$ be in the Sobolev space $H^k, k > 1$.

We will assume the support of $\hat{u}'$ to be $[-N : N]^2$ for some $N \in \mathbb{Z}^{>0}$, i.e. it shall be square and have an odd number of points in both directions. The purpose of these assumptions is to allow for a concise notation, but besides that they are of no importance for what is to follow. In concrete terms, we have $N \approx \frac{N_x}{2} = \frac{N_y}{2}$ for the Fourier discretization and $N \approx \rho_x 2^{J_x+1} = \rho_y 2^{J_y+1}$ for the ridgelet discretization where the $\approx$ accounts for rounding and small constant correction terms.

We write for the error

$$\begin{aligned}\|u - u'\|^2_{L^2(\Omega)} &:= \int_\Omega |u(x,y) - u'(x,y)|^2 \, dx \, dy \\ &= \sum_{(\hat{x},\hat{y}) \in \mathbb{Z}^2} |\hat{u}(\hat{x},\hat{y}) - \mathcal{Z}[\hat{u}'](\hat{x},\hat{y})|^2 \\ &= \sum_{(\hat{x},\hat{y}) \in \mathbb{Z}^2 \setminus [-N:N]^2} |\hat{u}(\hat{x},\hat{y})|^2 + \sum_{(\hat{x},\hat{y}) \in [-N:N]^2} |\hat{u}(\hat{x},\hat{y}) - \hat{u}'(\hat{x},\hat{y})|^2 \end{aligned} \tag{5.2.1}$$

where in the first line we made us of the Plancherel formula 2.3.6.

The first term describes a truncation error, thus by Theorem 2.4.7

$$\sum_{(\hat{x},\hat{y}) \in \mathbb{Z}^2 \setminus [-N:N]^2} |\hat{u}(\hat{x},\hat{y})|^2 = O\left(\frac{1}{N^{2k-1-\varepsilon}}\right)$$

for all $\varepsilon \in (0, 2k-1)$.

In order to estimate the second term in (5.2), we will need the following theorem.

**Theorem 5.2.1.** *Let $A \in \mathbb{R}^{n \times n}$ a nonsingular matrix and $\delta A \in \mathbb{R}^{n \times n}$ be such that $\|A^{-1}\|\|\delta A\| < 1$. Then, if $x \in \mathbb{R}^n$ is the solution of $Ax = b$ with $b \in \mathbb{R}^n$, $(b \neq 0)$ and $\delta x \in \mathbb{R}^n$ satisfies $(A + \delta A)(x + \delta x) = b + \delta b$ for $\delta \in \mathbb{R}^n$,*

$$\frac{\|\delta x\|}{\|x\|} \leq \frac{\kappa(A)}{1 - \kappa(A)\frac{\|\delta A\|}{\|A\|}} \left(\frac{\|\delta A\|}{\|A\|} + \frac{\|\delta b\|}{\|b\|}\right)$$

*where $\kappa(A) := \|A^{-1}\|\|A\|$ denotes the condition number of $A$.*

*Proof.* See [6, Theorem 3.1]. □

The exact solution of the RTE satisfies

$$\left(\mathtt{D}_{\mathtt{Tfs}} \circ \mathcal{C} \circ \hat{\mathcal{T}} \circ \mathcal{Z}\right)[\mathcal{C}[\hat{u}]] = \left(\mathtt{D}_{\mathtt{Tfs}} \circ \mathcal{C} \circ \mathcal{F}\right)[f] - \left(\mathtt{D}_{\mathtt{Tfs}} \circ \mathcal{C} \circ \hat{\mathcal{T}}\right)[\hat{u} - (\mathcal{Z} \circ \mathcal{C})[\hat{u}]] \tag{5.2.2}$$

whereas the approximate solution satisfies

$$(\mathtt{D}_{\mathtt{Tfs}} \circ \mathtt{Tfs})[\hat{u}'] = \mathtt{D}_{\mathtt{Tfs}}[\mathtt{ft}[f]] \tag{5.2.3}$$

In the notation of the above theorem, we can define the exact operator as

$$A := \mathtt{D_{Tfs}} \circ \mathcal{C} \circ \hat{\mathcal{T}} \circ \mathcal{Z}$$

with perturbation

$$\delta A := \mathtt{D_{Tfs}} \circ \mathtt{Tfs} - \mathtt{D_{Tfs}} \circ \mathcal{C} \circ \hat{\mathcal{T}} \circ \mathcal{Z}$$

and the exact right hand side as

$$b = \left(\mathtt{D_{Tfs}} \circ \mathcal{C} \circ \mathcal{F}\right)[f] - \left(\mathtt{D_{Tfs}} \circ \mathcal{C} \circ \hat{\mathcal{T}}\right)[\hat{u} - (\mathcal{Z} \circ \mathcal{C})[\hat{u}]]$$

with perturbation

$$\delta b := \mathtt{D_{Tfs}}[\mathtt{ft}[f]] - \left(\mathtt{D_{Tfs}} \circ \mathcal{C} \circ \mathcal{F}\right)[f] + \left(\mathtt{D_{Tfs}} \circ \mathcal{C} \circ \hat{\mathcal{T}}\right)[\hat{u} - (\mathcal{Z} \circ \mathcal{C})[\hat{u}]]$$

such that (5.2) and (5.2) become

$$A[\mathcal{C}[\hat{u}]] = b$$

and

$$(A + \delta A)\left[\hat{u}'\right] = b + \delta b$$

It is easy to verify that $\kappa(A)$, $\|A\|_{\hat{\Omega}_F}$ and $\|b\|_{\hat{\Omega}_F}$ are bounded in $N$. Also, we will prove soon that $\|\delta A\|_{\hat{\Omega}_F}$ vanishes for $N \to \infty$. In that limit, we thus have

$$\sum_{(\hat{x},\hat{y}) \in [-N:N]^2} |\hat{u}(\hat{x},\hat{y}) - \hat{u}'(\hat{x},\hat{y})|^2 = \|\mathcal{C}[\hat{u}] - \hat{u}'\|_{\hat{\Omega}_F}^2 = O\left(\|\delta A\|_{\hat{\Omega}_F} + \|\delta b\|_{\hat{\Omega}_F}\right)^2$$

Giving $\|\delta A\|_{\hat{\Omega}_F}$ a closer look, we get

$$\begin{aligned}
\|\delta A\|_{\hat{\Omega}_F} &= \max_{\substack{\hat{g}:[-N:N]^2 \to \mathbb{C} \\ \|\hat{g}\|_{\hat{\Omega}_F}=1}} \|\mathtt{D_{Tfs}}\left[\mathtt{Tfs}[\hat{g}] - \left(\mathcal{C} \circ \hat{\mathcal{T}} \circ \mathcal{Z}\right)[\hat{g}]\right]\|_{\hat{\Omega}_F} \\
&= \max_{\substack{\hat{g}:[-N:N]^2 \to \mathbb{C} \\ \|\hat{g}\|_{\hat{\Omega}_F}=1}} \|\mathtt{D_{Tfs}}\left[\mathtt{ft}\left[\kappa\, \mathtt{ift}[\hat{g}]\right] - (\mathcal{C} \circ \mathcal{F})\left[\kappa\, \left(\mathcal{F}^{-1} \circ \mathcal{Z}\right)[\hat{g}]\right]\right]\|_{\hat{\Omega}_F}
\end{aligned}$$

Using $\mathcal{F}^{-1} \circ \mathcal{Z} = \mathtt{ift}$, $\|\mathtt{D_{Tfs}}\|_{\hat{\Omega}_F} = 1$ and the convergence estimate for the quadrature error 2.4.9, we may continue

$$\begin{aligned}
\|\delta A\|_{\hat{\Omega}_F} &= \max_{\substack{\hat{g}:[-N:N]^2 \to \mathbb{C} \\ \|\hat{g}\|_{\hat{\Omega}_F}=1}} \|\mathtt{D_{Tfs}}\left[\mathtt{ft}\left[\kappa\, \mathtt{ift}[\hat{g}]\right] - (\mathcal{C} \circ \mathcal{F})\left[\kappa\, \mathtt{ift}[\hat{g}]\right]\right]\|_{\hat{\Omega}_F} \\
&\leq \max_{\substack{\hat{g}:[-N:N]^2 \to \mathbb{C} \\ \|\hat{g}\|_{\hat{\Omega}_F}=1}} \|\mathtt{D_{Tfs}}\|_{\hat{\Omega}_F} \|\mathtt{ft}\left[\kappa\, \mathtt{ift}[\hat{g}]\right] - (\mathcal{C} \circ \mathcal{F})\left[\kappa\, \mathtt{ift}[\hat{g}]\right]\|_{\hat{\Omega}_F} \\
&= \max_{\substack{\hat{g}:[-N:N]^2 \to \mathbb{C} \\ \|\hat{g}\|_{\hat{\Omega}_F}=1}} O\left(N^{-(k-1)}\right) \\
&= O\left(N^{-(k-1)}\right)
\end{aligned}$$

Similarly, we get for $\|\delta b\|_{\hat{\Omega}_F}$

$$\begin{aligned}\|\delta b\|_{\hat{\Omega}_F} &= \|\mathtt{D_{Tfs}}\left[\mathtt{ft}[f] - (\mathcal{C}\circ\mathcal{F})\left[f\right]\right] + \left(\mathtt{D_{Tfs}}\circ\mathcal{C}\circ\hat{\mathcal{T}}\right)\left[\hat{u} - (\mathcal{Z}\circ\mathcal{C})\left[\hat{u}\right]\right]\|_{\hat{\Omega}_F} \\ &\leq \|\mathtt{D_{Tfs}}\|_{\hat{\Omega}_F}\|\mathtt{ft}[f] - (\mathcal{C}\circ\mathcal{F})\left[f\right]\|_{\hat{\Omega}_F} + \|\left(\mathtt{D_{Tfs}}\circ\mathcal{C}\circ\hat{\mathcal{T}}\right)\left[\hat{u} - (\mathcal{Z}\circ\mathcal{C})\left[\hat{u}\right]\right]\|_{\hat{\Omega}_F}\end{aligned}$$

For the first term, the same arguments as we used when estimating $\|\delta A\|_{\hat{\Omega}_F}$ apply. For the second term, we have by Theorem 2.4.7 that $\|\hat{u}-(\mathcal{Z}\circ\mathcal{C})\left[\hat{u}\right]\|_{\hat{\Omega}_F} = O\left(N^{-(k-1/2-\varepsilon/2)}\right)$. Since $\mathtt{D_{Tfs}}\circ\mathcal{C}\circ\hat{\mathcal{T}}$ is a bounded operator, we thus get

$$\begin{aligned}\|\delta b\|_{\hat{\Omega}_F} &= O\left(N^{-(k-1)}\right) + O(1)\,O\left(N^{-(k-1/2-\varepsilon/2)}\right) \\ &= O\left(N^{-(k-1)}\right)\end{aligned}$$

In conclusion,

$$\sum_{(\hat{x},\hat{y})\in[-N:N]^2} |\hat{u}(\hat{x},\hat{y}) - \hat{u}'(\hat{x},\hat{y})|^2 = O\left(\|\delta A\|_{\hat{\Omega}_F} + \|\delta b\|_{\hat{\Omega}_F}\right)^2 = O\left(N^{-2(k-1)}\right)$$

Inserting our results into equation (5.2), we see that the convergence of the basic RTE solvers is

$$\|u-u'\|^2_{L^2(\Omega)} = O\left(N^{-(2k-1-\varepsilon)}\right) + O\left(N^{-2(k-1)}\right) = O\left(N^{-2(k-1)}\right)$$

i.e.

$$\|u-u'\|_{L^2(\Omega)} = O\left(N^{-(k-1)}\right)$$

or specifically for the ridgelet based discretization (assuming $J_x = J_y =: J$)

$$\|u-u'\|_{L^2(\Omega)} = O\left(2^{-J(k-1)}\right)$$

## 5.3 Discrete Ordinates Method

As a next step, we consider the same equation

$$s\cdot\nabla u + \kappa\, u = f \tag{5.3.1}$$

but this time we let $s\in\mathbb{S}^1$ also be an independent variable such that $u,\kappa,f:\Omega\times\mathbb{S}^1\to\mathbb{R}$. The *discrete ordinates method* (DOM) as outlined in [8, Section 2] solves this problem in the following way:

- Choose some directions $\{s_i\}_{i=1}^{N_s}\subset\mathbb{S}^1, N_s\in\mathbb{Z}^{\geq 1}$.
- Solve (5.3) for these fixed directions, which gives you the one-directional solutions $u'_i(x,y)$.

- Interpolate the $(s_i, u'_i)$ to get a solution for the full domain $\Omega \times \mathbb{S}^1$.

In this report, we will use equispaced directions $s_i := 2\pi \frac{i-1}{N}$ and linear interpolation for simplicity. Step two is done with the ridgelet based solver developed in the previous section.

Introducing the equispaced periodic linear interpolation operator

$$\overset{N}{\underset{i=1}{\boldsymbol{\mathcal{I}}_S}} [f_i](x,y,s) := \begin{cases} f_{l+1}(x,y) & \text{if } l := \frac{N\varphi(s)}{2\pi} \in \mathbb{Z} \\ (\lceil l \rceil - l) f_{\lfloor i \rfloor + 1}(x,y) + \dots \\ \quad (l - \lfloor l \rfloor) f_{(\lceil l \rceil \bmod N)+1}(x,y) & \text{otherwise} \end{cases}$$

($\varphi(s)$ denotes the angle between $s \in \mathbb{S}^1$ and the positive $x$-axis in the usual mathematical convention), we can write the solution $u'$ produced by the DOM as

$$u'(x,y,s) = \overset{N_s}{\underset{i=1}{\boldsymbol{\mathcal{I}}_S}} [u'_i](x,y,s)$$

If we further let $u : \Omega \times \mathbb{S}^1$ be the exact solution and $\delta u_i(x,y) := u(x,y,s_i) - u'_i(x,y)$ the error in the approximate solutions $u'_i$, we get for the total error

$$\begin{aligned} \left\| u - u' \right\|_{L^2(\Omega \times \mathbb{S}^1)} &= \left\| u - \overset{N_s}{\underset{i=1}{\boldsymbol{\mathcal{I}}_S}} [u_i + \delta u_i] \right\|_{L^2(\Omega \times \mathbb{S}^1)} \\ &\leq \left\| u - \overset{N_s}{\underset{i=1}{\boldsymbol{\mathcal{I}}_S}} [u_i] \right\|_{L^2(\Omega \times \mathbb{S}^1)} + \left\| \overset{N_s}{\underset{i=1}{\boldsymbol{\mathcal{I}}_S}} [\delta u_i] \right\|_{L^2(\Omega \times \mathbb{S}^1)} \end{aligned}$$

The first term describes a pure interpolation error, which for linear interpolation is known to be $O\left(N_s^{-2}\right)$ if $u(x,y,\cdot) \in C^2$. The second term is the error due to the basic RTE solver, which in the previous section was shown to be $O\left(2^{-J(k-1)}\right)$. In conclusion, we thus have

$$\|u - u'\|_{L^2(\Omega \times \mathbb{S}^1)} = O\left(N_s^{-2}\right) + O\left(2^{-J(k-1)}\right)$$

As we can see, we have to choose $N_s \sim b^J$ with $b = 2^{-\frac{1}{2}(k-1)}$ in order for the angular and spatial errors to be balanced. The outlined discrete ordinates method scales thus as $O\left(N_s\, 2^{J_x + J_y}\right) = O\left((4b)^J\right)$, which can quickly become prohibitively expensive.

## 5.4 Sparse Discrete Ordinates Method

In order to mitigate the scaling problem of the (full) discrete ordinates method, the *sparse discrete ordinates method* (SDOM) was developed in [8, Section 4]. Adapted to the situation here, the SDOM reads the following: Given a finite ridgelet frame with $J_x = J_y =: J$ and a constant $b \in \mathbb{Z}^{\geq 2}$, let $j = 1, ..., J$ and $i = 1, ..., b^{J-j+1}$. Then, for each pair $(j,i)$, we solve the RTE in direction $s_{j,i} := \left(\cos\left(2\pi \frac{i-1}{b^{J-j+1}}\right), \sin\left(2\pi \frac{i-1}{b^{J-j+1}}\right)\right)^T$ using the ridgelet RTE solver developed in Section 5.1 with a subframe of the original

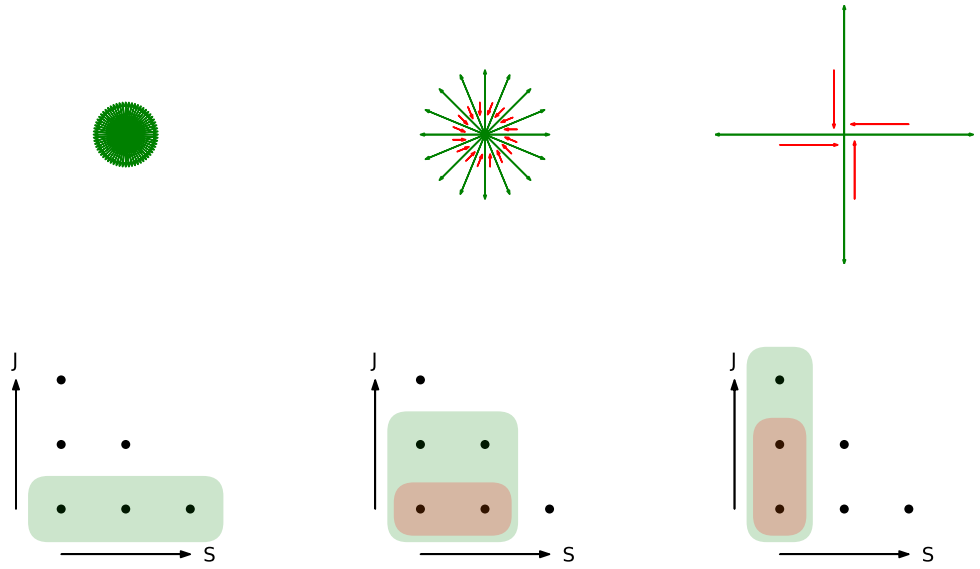


Figure 5.1: Illustration of the SDOM for $J = 3$ and $b = 4$. In the upper row, the lengths of the arrows represent the number of scales that were used whereas their number and directions indicate how many and which directions are used for angular interpolation. The bottom row shows in which detail spaces the functions obtained in this way live (the J-arrow denotes increasing frame size, the S-arrow denotes increasing number of angular interpolation points).

frame where $J_x = J_y = j$. These partial solutions are stored in $u'_{j,i}(x, y)$ and eventually the full solution $u'(x, y, s)$ is computed as

$$u'(x,y,s) = \overset{b^J}{\underset{i=1}{\boldsymbol{\mathcal{I}}_S}} \left[u'_{1,i}\right](x,y,s) + \ldots \\ \sum_{j=2}^{J} \left( \overset{b^{J-j+1}}{\underset{i=1}{\boldsymbol{\mathcal{I}}_S}} \left[u'_{j,i}\right](x,y,s) - \overset{b^{J-j+1}}{\underset{i=1}{\boldsymbol{\mathcal{I}}_S}} \left[u'_{j-1,\,b\,(i-1)+1}\right](x,y,s) \right)$$

A graphical representation of the SDOM is given in Figure 5.1.

In [8, Lemma 4.3], Grella and Schwab show that in their setting the convergence of the SDOM deteriorates only by a logarithmic factor compared to the full DOM with physical and angular resolutions equal to the *highest* resolutions used in the SDOM. The same proof works in our case as well, but since the basic RTE solver is not a mere projection of the true solution to some subspace, our notation will be somewhat different.

Let $u : \Omega \times \mathbb{S}^1$ be the exact solution and $\delta u_{j,i}(x, y) := u(x, y, s_i) - u'_{j,i}(x, y)$. Furthermore, let $\delta u_j(x, y, s) := u(x, y, s) - u'_j(x, y, s)$ where $u'_j$ is the solution obtained with the

basic RTE solver in *any* direction $s \in \mathbb{S}^1$. We can then write

$$\|u - u'\|_{L^2(\Omega\times\mathbb{S}^1)} = \Bigg\| u - \overset{b^J}{\underset{i=1}{\boldsymbol{\mathcal{I}}_S}} \left[u(s_{1,i}) + \delta u_{1,i}\right] - \dots \\ \sum_{j=2}^{J} \left( \overset{b^{J-j+1}}{\underset{i=1}{\boldsymbol{\mathcal{I}}_S}} \left[u(s_{j,i}) + \delta u_{j,i}\right] - \overset{b^{J-j+1}}{\underset{i=1}{\boldsymbol{\mathcal{I}}_S}} \left[u(s_{j-1,b\,(i-1)+1}) + \delta u_{j-1,b\,(i-1)+1}\right] \right) \Bigg\|_{L^2(\Omega\times\mathbb{S}^1)}$$

where $u(s)$ is a shorthand notation for $u(\cdot,\cdot,s)$. Since $s_{j,i} = s_{j,b\,(i-1)+1}$, the $u$ in the sum cancel, and the remaining terms can be rearranged to

$$\begin{aligned} \|u - u'\|_{L^2(\Omega\times\mathbb{S}^1)} &\leq \left\| u - \overset{b^J}{\underset{i=1}{\boldsymbol{\mathcal{I}}_S}} u(s_{1,i}) \right\|_{L^2(\Omega\times\mathbb{S}^1)} + \dots \\ &\qquad \sum_{j=1}^{J-1} \left\| \overset{b^{J-j+1}}{\underset{i=1}{\boldsymbol{\mathcal{I}}_S}} \delta u_{j,i} - \overset{b^{J-j}}{\underset{i=1}{\boldsymbol{\mathcal{I}}_S}} \delta u_{j,b\,(i-1)+1} \right\|_{L^2(\Omega\times\mathbb{S}^1)} + \left\| \overset{b}{\underset{i=1}{\boldsymbol{\mathcal{I}}_S}} \delta u_{J,i} \right\|_{L^2(\Omega\times\mathbb{S}^1)} \\ &\leq \left\| u - \overset{b^J}{\underset{i=1}{\boldsymbol{\mathcal{I}}_S}} u(s_{1,i}) \right\|_{L^2(\Omega\times\mathbb{S}^1)} + \sum_{j=1}^{J-1} \left\| \delta u_j - \overset{b^{J-j+1}}{\underset{i=1}{\boldsymbol{\mathcal{I}}_S}} \delta u_{j,i} \right\|_{L^2(\Omega\times\mathbb{S}^1)} + \dots \\ &\qquad \sum_{j=1}^{J-1} \left\| \delta u_j - \overset{b^{J-j}}{\underset{i=1}{\boldsymbol{\mathcal{I}}_S}} \delta u_{j,b\,(i-1)+1} \right\|_{L^2(\Omega\times\mathbb{S}^1)} + \left\| \overset{b}{\underset{i=1}{\boldsymbol{\mathcal{I}}_S}} \delta u_{J,i} \right\|_{L^2(\Omega\times\mathbb{S}^1)} \end{aligned}$$

Inserting the known convergence rates for linear interpolation and the basic RTE solver, and estimating the sums by their largest term, we get

$$\begin{aligned} \|u - u'\|_{L^2(\Omega\times\mathbb{S}^1)} &= O\left(b^{-2J}\right) + \sum_{j=1}^{J-1} O\left(b^{-2(J-j+1)}\right) O\left(2^{-j(k-1)}\right) + \dots \\ &\qquad \sum_{j=1}^{J-1} O\left(b^{-2(J-j)}\right) O\left(2^{-j(k-1)}\right) + O\left(2^{-J(k-1)}\right) \\ &= O\left(J\left(b^{-2J} + 2^{-J(k-1)}\right)\right) \end{aligned}$$

Note that for this estimate to work, we have to assume the solution $u$ *and* the error functions $\delta u_j$ to be at least $C^2$ in $s$. Compared to the convergence estimate for the DOM which only required $u \in C^2(\mathbb{S}^1)$, we thus have one additional smoothness assumption for the SDOM. Since we know only very little about the structure of the error functions, it is not a priori clear whether they exhibit the required smoothness properties even in the case when the solution $u$ does. We will come back to this issue when discussing numerical findings in Section 6.4.

The following complexity estimate is nothing but a reformulation of [8, Lemma 3.1].

**Theorem 5.4.1** (Complexity of SDOM)**.** *The number of degrees of freedoms in the SDOM is* $O\left(J^{\delta_{b,4}} \max\{b,4\}^J\right)$.

*Proof.* Simply sum the numbers of degrees of freedom of the $u_{j,i}$:

$$\sum_{j=1}^{J} b^{J-j+1}\, O(4^j) = O\left(b^{J+1} \sum_{j=1}^{J} \left(\frac{4}{b}\right)^j\right)$$

If we assume $b \neq 4$, we can continue with

$$O\left(b^{J+1} \sum_{j=1}^{J} \left(\frac{4}{b}\right)^j\right) = O\left(\frac{4^{J+1} - b^{J+1}}{4-b}\right) = O\left(\max\{b,4\}^J\right)$$

Otherwise, we get

$$O\left(b^{J+1} \sum_{j=1}^{J} \left(\frac{4}{b}\right)^j\right) = O\left(J\, 4^J\right)$$

□

Thus, if we assume the above convergence estimate to be correct, we see that the SDOM achieves a speedup of

$$\frac{\frac{O\left(J^{\delta_{b,4}} \max\{b,4\}^J\right)}{O\left(J\left(b^{-2J}+2^{-J(k-1)}\right)\right)}}{\frac{O((4b)^J)}{O\left(b^{-2J}+2^{-J(k-1)}\right)}} = O\left(\frac{\min\{b,4\}^J}{J^{1+\delta_{b,4}}}\right)$$

as compared to the DOM.

## 5.5 Source Iterations

Finally, we are able to tackle the complete RTE including the scattering term:

$$s \cdot \nabla u + \kappa\, u = f + \int_{\mathbb{S}^1} \sigma u \, ds'$$

This problem can be solved using the *source iteration* method, which is:

- Set $u'^{(0)}(x,y,s) = 0$.
- For $t = 1, ..., T$, solve

$$s \cdot \nabla u'^{(t)} + \kappa\, u'^{(t)} = f + \int_{\mathbb{S}^1} \sigma u'^{(t-1)} \, ds'$$

  using e.g. the DOM or SDOM based on the basic ridgelet RTE solver.

Obviously, the idea of the source iterations is that the $u^{(t)}$ will converge to the true solution $u$ for large enough $t$. We are not aware of any mathematical results proving this convergence or giving some estimates on the speed of convergence, but the numerical findings presented in Section 6.5 will show that this method works fairly well.

# 6 Numerical Experiments

Some parameters of the previously developed theory remain constant throughout this chapter. In order to avoid repeating them over and over again, we introduce them here:

- The real space domain is the unit square $\Omega = [0,1]^2$ (i.e. $L_x = L_y = 1$)
- Square frames with $J_x = J_y = J$, $\rho_x = \rho_y = 1$ and square finite Fourier spaces with $N_x = N_y = N$ are used.
- The radial and spherical shape functions for the ridgelets are

$$\psi_{Radial}(x) = \sin\left(\frac{\pi}{2}\, v(x)\right)$$

$$\psi_{Spherical}(x) = \sqrt{v(1-x)}$$

  with the helper polynomial $v : [0,1] \to [0,1]$ given by

$$v(x) := 35x^4 - 84x^5 + 70x^6 - 20x^7$$

  This choice is very similar to the one made in [2], which in turn took the polynomial $v$ from [3].

- Since three-dimensional functions are difficult to visualize, we will only look at the *incident radiation*

$$G[u](x,y) := \int_{\mathbb{S}^1} u(x,y,s)\, ds$$

  when solving the multi-directional RTE. Note that both the DOM and SDOM produce solutions which are piecewise linear in $s$, therefore we can compute the above integral exactly for these functions.

## 6.1 Convergence Of CG

The speed of the basic solver presented in Section 5.1 depends crucially on how fast the CG iterations converge. Therefore, we investigate the convergence of this method when applied to equations (5.1) and (5.1).

From theory we know that the error $e_k := \|x_k - A^{-1}b\|$ in the $k$-th CG iterand $x_k$ decays with $O(\rho_{CG}^k)$ where the *error reduction constant* $\rho_{CG}$ is given by

$$\rho_{CG} = \frac{\sqrt{\kappa_{CG}} - 1}{\sqrt{\kappa_{CG}} + 1}$$

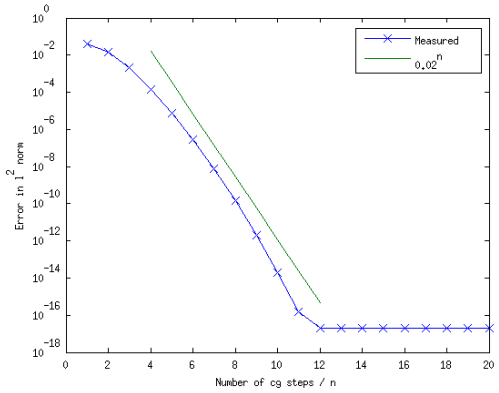


(a) $\varphi = 0$

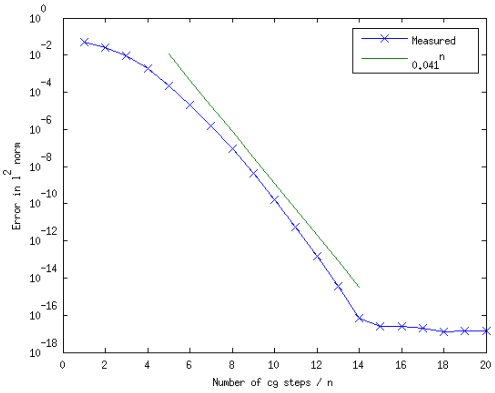


(b) $\varphi = \frac{\pi}{4}$

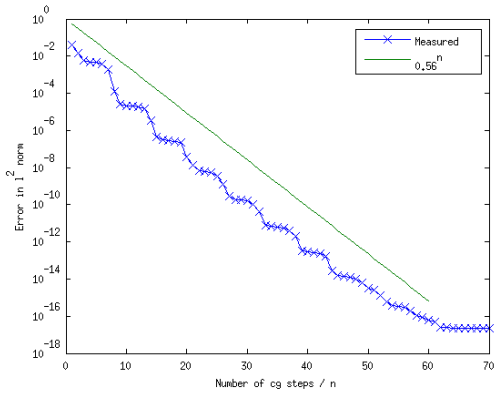


(c) $\varphi = 0.01$

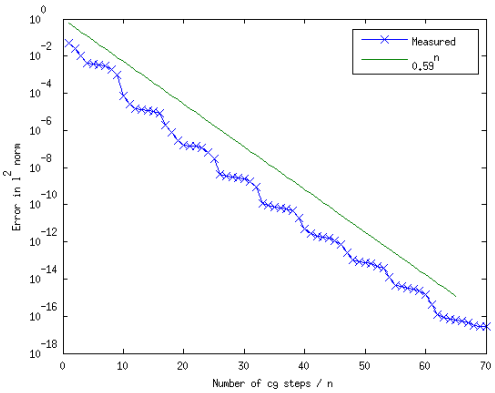


(d) $\varphi = \frac{\pi}{4} - 0.01$

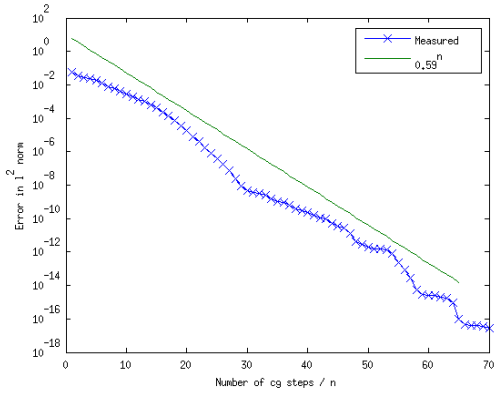


(e) $\varphi = 0.1$

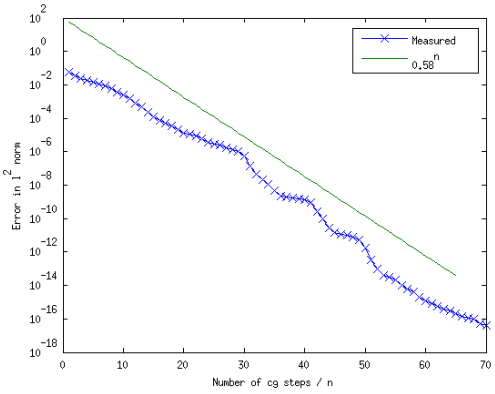


(f) $\varphi = \frac{\pi}{4} - 0.1$

Figure 6.1: Convergence of CG applied to the Fourier space RTE (5.1) using $N = 64$, $s = (\cos(\phi), \sin(\phi))^T$, $\kappa = 1$ and $f(x, y) = e^{-100((x-0.5)^2+(y-0.5)^2)}$. The condition number is bounded by $1 + 4\pi^2 \approx 40.5$ which gives an expected rate of convergence of $\rho_{CG} \approx 0.73$.

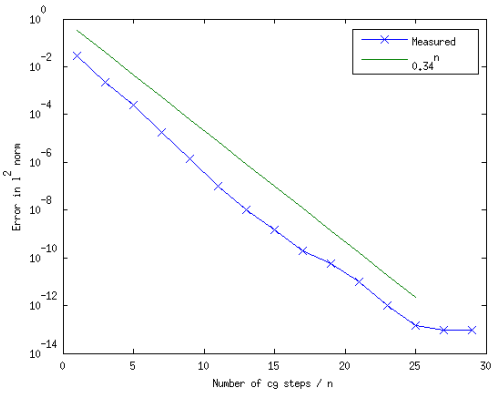


(a) $\varphi = 0$

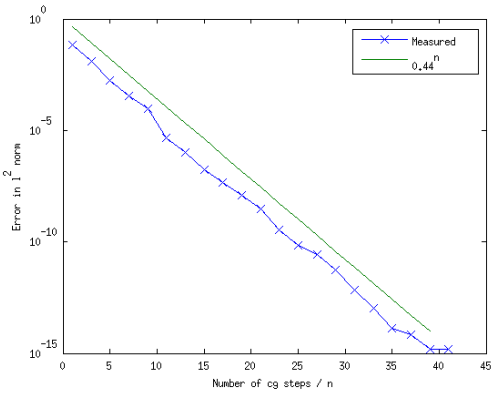


(b) $\varphi = \frac{\pi}{4}$

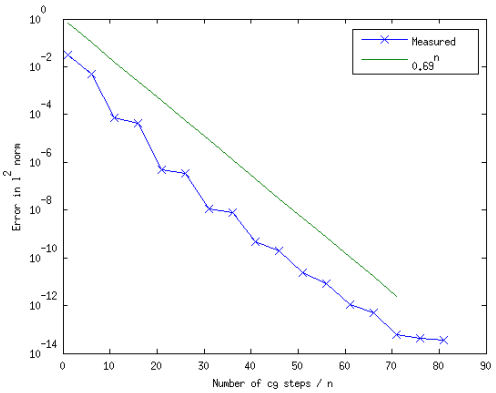


(c) $\varphi = 0.01$

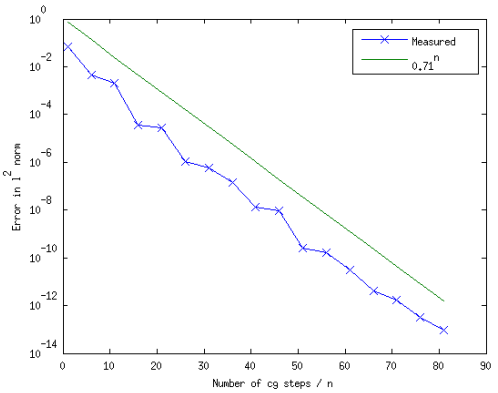


(d) $\varphi = \frac{\pi}{4} - 0.01$

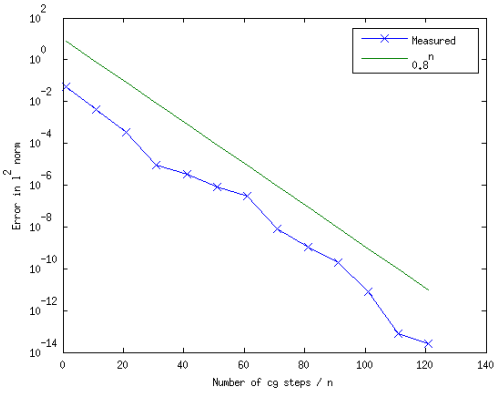


(e) $\varphi = 0.1$

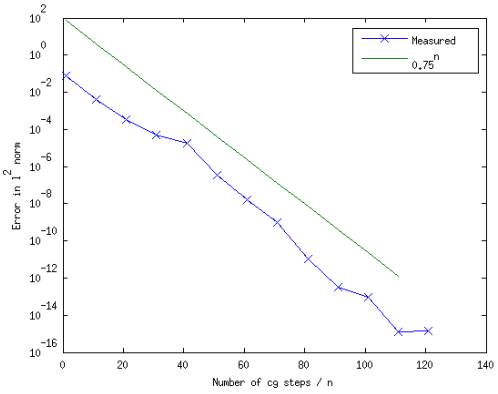


(f) $\varphi = \frac{\pi}{4} - 0.1$

Figure 6.2: Convergence of CG applied to the ridgelet space RTE (5.1) using $J = 4$, $s = (\cos(\phi), \sin(\phi))^T$, $\kappa = 1$ and $f(x, y) = e^{-100((x-0.5)^2+(y-0.5)^2)}$.

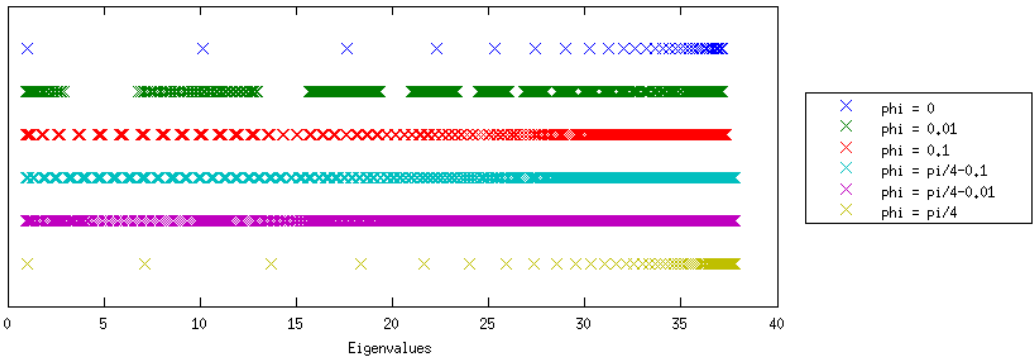


Figure 6.3: Eigenvalues of $\mathtt{D_{Tfs}} \circ \mathtt{Tfs}^* \circ \mathtt{Tfs} \circ \mathtt{D_{Tfs}}$ for $N_x = N_y = 64$, $\kappa = 1$ and $s = (\cos(\phi), \sin(\phi))^T$.

($\kappa_{CG}$ denotes the condition number $\kappa_{CG} := \|A\|\|A^{-1}\|$.) In the case of constant absorption coefficient $\kappa$, the operator used in the Fourier space RTE (5.1) becomes diagonal and can be analytically computed.

$$(\mathtt{D_{Tfs}} \circ \mathtt{Tfs}^* \circ \mathtt{Tfs} \circ \mathtt{D_{Tfs}})\,[\hat{f}](\hat{x},\hat{y}) = d\,(\alpha(\hat{x},\hat{y}))\,\hat{f}(\hat{x},\hat{y})$$
$$\text{with} \quad \alpha(\hat{x},\hat{y}) := s \cdot (\hat{x},\hat{y})^T, \quad d(\alpha) := \frac{(2\pi\alpha)^2 + \kappa^2}{(1+|\alpha|)^2}$$

Therefore, also bounds for the condition number can be analytically computed.

$$\kappa_{CG} \leq \frac{\max\limits_{\alpha\in\mathbb{R}} d(\alpha)}{\min\limits_{\alpha\in\mathbb{R}} d(\alpha)} = 1 + \max\left\{\frac{\kappa^2}{4\pi^2}, \frac{4\pi^2}{\kappa^2}\right\}$$

The ridgelet preconditioner (5.1) can be viewed as a coarser version of the Fourier one (5.1), thus one expects the condition number for the ridgelet RTE (5.1) to be worse but similar to the one shown above.

In conclusion, the above theory tells us that the rate of convergence of the CG method depends on the absorption coefficient $\kappa$, which is what we observe in practice. However, Figures 6.1 and 6.2 show that the rate of convergence also depends heavily on the transport direction $s$: If we transport along the axes or diagonals, the convergence rate is *much* faster than what theory predicts, while otherwise the theoretical bound is quite sharp (often even sharper than what is shown in Figure 6.1). A possible explanation for this behaviour could be the clustering of eigenvalues: CG is known to converge much faster if the eigenvalues of the coefficient matrix are clustered around some few points [9]. In our case, this situation occurs if we let e.g. $s = (1,0)^T$, because then all Fourier space points with same $\hat{x}$ lead to the same eigenvalue $d(\hat{x})$. On the other hand, if the greatest common divisor of $s_x$ and $s_y$ is very small (or even inexistent), $\alpha$ attains a lot more values and so the eigenvalues are scattered over the entire range. Figure 6.3 nicely shows this for the operators encountered in Figure 6.1.

## 6.2 Convergence Of Basic RTE Solver

We tested the convergence theory from Section 5.2 with the following scheme:

- Fix $\kappa$ and $s$ to some constant value ($\kappa = 8$ and $s = (1, 0)^T$ in our case)
- Construct a polynomial solution $u$ with known smoothness $H^k$ across the boundary of $[0, 1]^2$
- Compute $f$ for the chosen values of $\kappa$, $s$ and $u$.
- Estimate the convergence rate $\rho$ such that the error of the ridgelet based RTE solver is approximately $O\left(\rho^J\right)$ for $J = 0, ..., 5$

In this way, we obtained the following convergence rates:

| $k$ | 2 | 3 | 4 | 5 |
|---|---|---|---|---|
| $\rho$ | 0.53 | 0.25 | 0.086 | 0.058 |

The $\rho$ for $k = 2, 3, 5$ agree with the predicted $\rho = 2^{-(k-1)}$ with reasonable accuracy. The convergence rate for $k = 4$ is actually closer to the one predicted for $k = 4.5$ ($2^{-(4.5-1)} \approx 0.088$). The reason for this deviation is unclear, yet it does not contradict our theoretical findings and the result for $k = 5$ shows that there is no systematic deviation.

Figure 6.4 gives further examples of convergence rates. In particular, Figure 6.4b shows that the magnitude of the jump in one of the derivatives influences the convergence rate as well: If we increase the jump in $\kappa$, the kink in $u$ at $x = 0.4$ becomes more pronounced and the convergence rates approaches $\rho = 0.5$. If the kink in $u$ is only small, however, the convergence rate can be significantly better.

## 6.3 General Dirichlet Boundary Conditions

Assuming that $\kappa$ and $f$ are constant in the transport direction $s$, it is easily checked that the solution of the mono-directional RTE

$$s \cdot u + \kappa\, u = f$$

is given by

$$u(x, y) = A(x, y)\, e^{-\kappa\, s \cdot (x,y)^T} + \frac{f}{\kappa} \tag{6.3.1}$$

where $A(x, y)$ is a function determined by the boundary conditions which may only vary in the direction orthogonal to $s$. This result can be used to generalize the basic RTE solvers from Section 5.1 which require periodic boundaries to arbitrary Dirichlet boundary conditions as follows.

Assume we want to impose Dirichlet boundary conditions

$$u(x, y) = \Gamma(x, y)$$

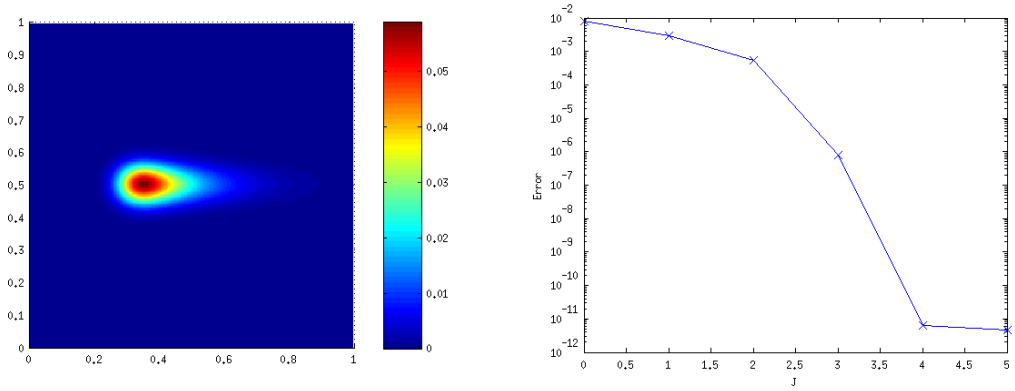


(a) $s = (1,0)^T$, $\kappa = 8$, $f(x,y) = e^{-300\left((x-0.3)^2+(y-0.5)^2\right)}$

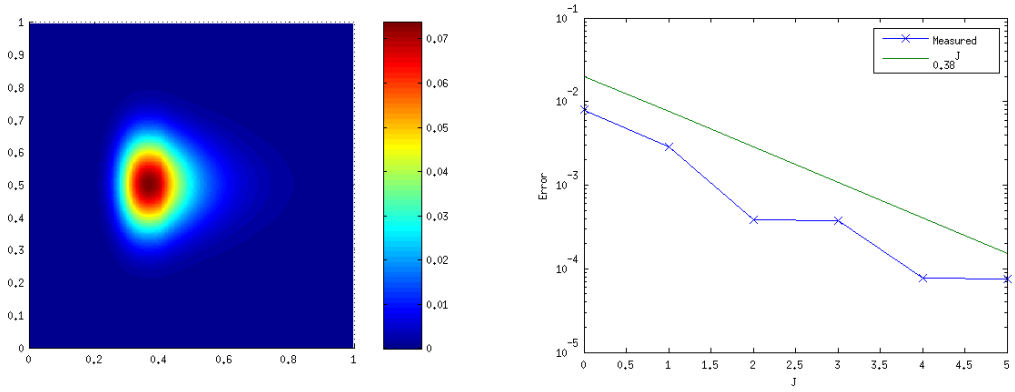


(b) $s = (1,0)^T$, $\kappa = \begin{cases} 4 & x \leq 0.4 \\ 10 & \text{otherwise} \end{cases}$, $f(x,y) = e^{-300\,(x-0.3)^2-50\,(y-0.5)^2}$

Figure 6.4: (Continued on next page)

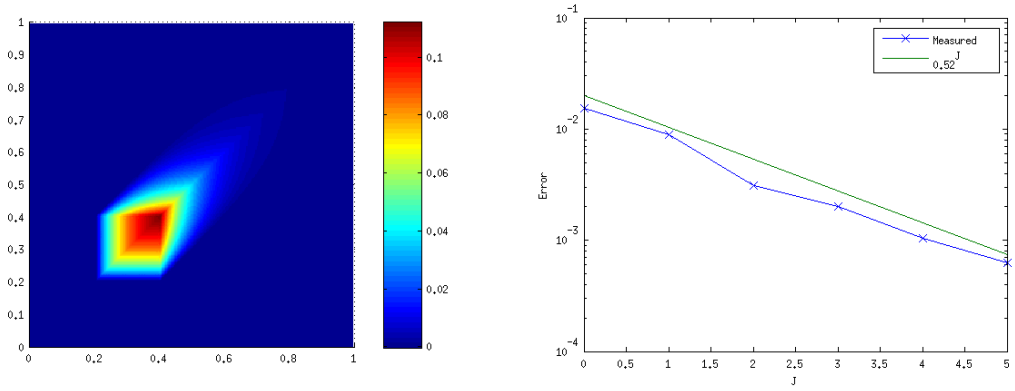


(c) $s = \frac{1}{\sqrt{2}}(1,1)^T$, $\kappa = 8$, $f(x,y) = \begin{cases} 1 & |x-0.3| < 0.1 \wedge |y-0.3| < 0.1 \\ 0 & \text{otherwise} \end{cases}$

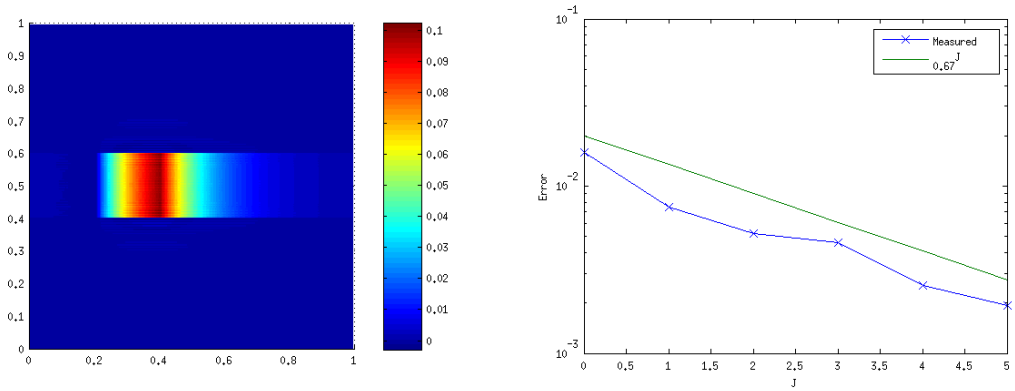


(d) $s = (1,0)^T$, $\kappa = 8$, $f(x,y) = \begin{cases} 1 & |x-0.3| < 0.1 \wedge |y-0.5| < 0.1 \\ 0 & \text{otherwise} \end{cases}$

Figure 6.4: Convergence of the ridgelet based basic method as a function of the frame size $J$. The error was computed as the difference in Fourier space norm to the "exact" solution obtained with $J = 6$, which is shown in real space on the left. CG iterations were aborted once either the relative residual (measured in ridgelet coefficient space) dropped below $10^{-8}$ or 100 iteration steps were executed.

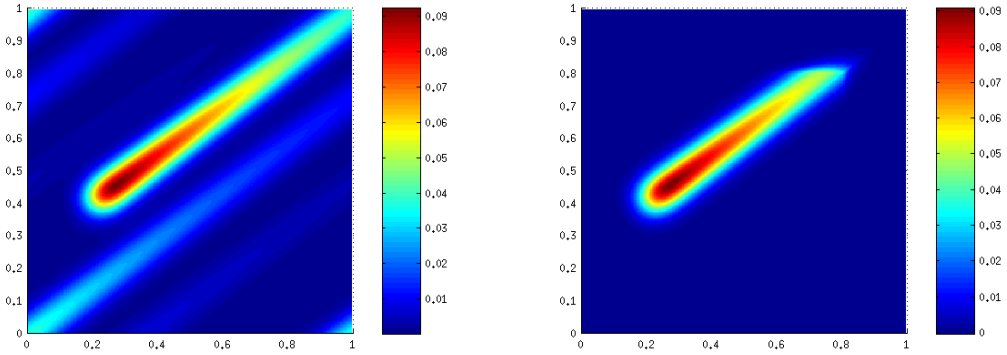

(a) Periodic boundaries on $[0,1]^2$ (b) Homogeneous boundaries on $[0,\ 0.8]^2$

Figure 6.5: Imposing homogeneous boundary conditions by increasing $\kappa$ near the boundaries. In both plots,

$$f(x,y) = e^{-300\left((x-0.2)^2+(y-0.4)^2\right)}$$

On the left, $\kappa(x,y) = 1$, whereas on the right

$$\kappa(x,y) = \begin{cases} 1 & x \leq 0.8 \wedge y \leq 0.8 \\ 30 & \text{otherwise} \end{cases}$$

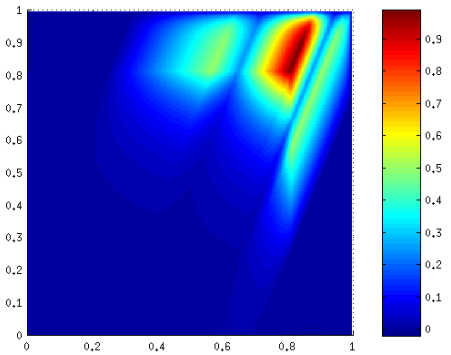

(a) Nonhomogenous boundaries on $[0, l]^2$

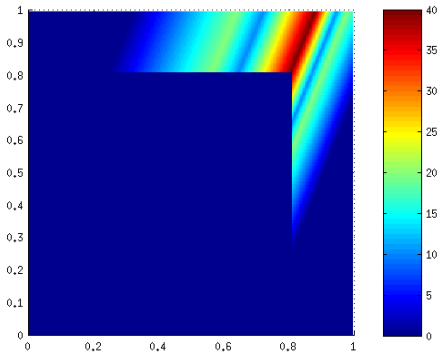

(b) Plot of the $f$ used in (a)

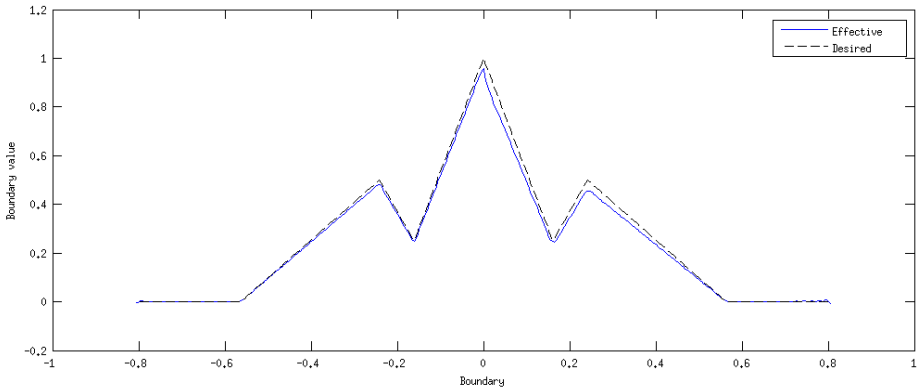


(c) Comparison between the effective boundary conditions and the desired ones. In the above plot, the negative half axis shows the cross section along the line from $(0, l)$ to $(l, l)$, and the positive half axis from $(l, l)$ to $(l, 0)$. The blue line shows the effective value of $u$, the dashed line the boundary conditions we wanted to impose.

Figure 6.6: Imposing nonhomogeneous boundary conditions by choosing suitable values for $\kappa$ and $f$ near the boundaries. $s \approx (-0.37, -0.93)^T$, i.e. the radiation is transported from top right to down left. The expression for $f$ is complicated, but the resulting function is shown in (b).

$$\kappa(x, y) = \begin{cases} 8 & x \leq l \wedge y \leq l \\ 40 & \text{otherwise} \end{cases}$$

with $l \approx 0.8047$. $l$ was chosen such that the inflow boundary lies on a grid point of the `ft`.

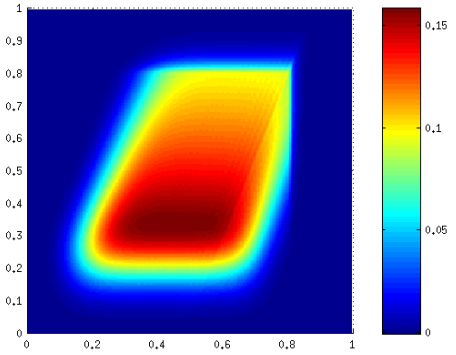

(a) Nonsmooth boundary

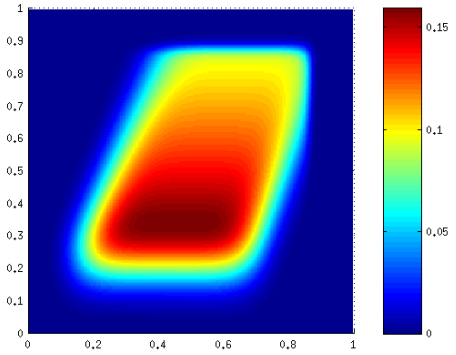

(b) Smooth boundary

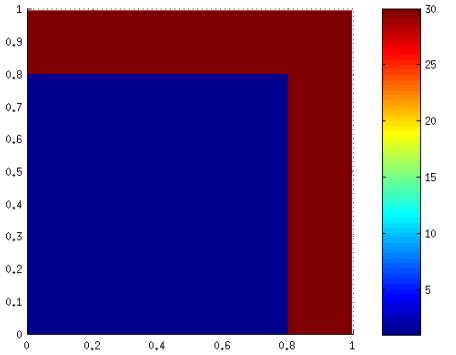

(c) Plot of the $\kappa$ used in (a)

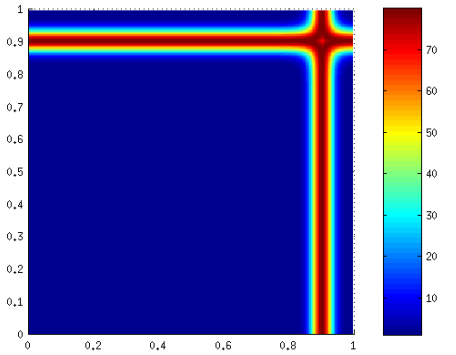

(d) Plot of the $\kappa$ used in (b)

Figure 6.7: Imposing homogeneous boundary conditions using a smooth boundary. In (a) and (b),

$$f(x,y) = e^{-2000\,(x-0.4)^6 - 100\,(y-0.2)^2}$$

In (a),

$$\kappa(x,y) = \begin{cases} 1 & x \leq 0.8 \wedge y \leq 0.8 \\ 30 & \text{otherwise} \end{cases}$$

whereas in (b)

$$\kappa(x,y) = 1 + 79\, e^{-\left(\frac{3}{5}\log(e^{-50\,|x-0.9|} + e^{-50\,|y-0.9|})\right)^2}$$

on the inflow boundary of $\Omega_{Dirichlet} := [0,l]^2$ where $l \in (0,1)$. In order to do so, we run the basic solvers on the larger domain $\Omega := [0,1]^2$. On the newly added $\Omega_{Boundary} := \Omega \setminus \Omega_{Dirichlet}$, we set $\kappa\,|_{\Omega_{Boundary}}$ to some (large) constant $\kappa_{Boundary}$, whereas

$$f(x,y) := \kappa_{Boundary}\,\Gamma(x + t\,s_x, y + t\,s_y)$$

for $(x,y) \in \Omega_{Boundary}$ and

$$t = \min\left\{ t' \in \mathbb{R}^{>0} \;\middle|\; \begin{array}{c}(x + t'\,s_x \bmod 1,\; y + t'\,s_y \bmod 1) \text{ lies on the} \\ \text{inflow boundary of } \Omega_{Dirichlet}\end{array} \right\}$$

With these choices, we get that $u\,|_{\Omega_{Boundary}}$ is of the same form as (6.3) where only $A(x,y)$ depends on the value of $u$ on the inflow boundary of $\Omega_{Boundary}$ (which is the same as the outflow boundary of $\Omega_{Dirichlet}$). The influence of the radiation leaving $\Omega_{Dirichlet}$ is thus reduced by a factor of at least $e^{-\kappa_{Boundary}(1-l)}$ before it enters $\Omega_{Dirichlet}$ again. The second term, on the other hand, is simply $\Gamma(x + t\,s_x, y + t\,s_y)$, so we see that we can impose the boundary conditions with arbitrary precision by choosing large enough values for $\kappa_{Boundary}$. This procedure is illustrated in Figures 6.5 and 6.6.

Of course, more complicated choices of $\kappa\,|_{\Omega_{Boundary}}$ and $f\,|_{\Omega_{Boundary}}$ are possible. Since jumps in $\kappa$ and $f$ limit the smoothness of the solution and thus the convergence of the method, it would for example be desirable to have them vary more smoothly across the boundaries of $\Omega_{Dirichlet}$. While it is hard to derive a recipe that gives smooth $\kappa$ and $f$ for all possible boundary conditions, important special cases like homogeneous boundary conditions are easy to impose with smooth parameters, see Figure 6.7.

## 6.4 Convergence Of SDOM Compared To DOM

When deriving the DOM and SDOM, we showed that their convergence estimates differ only in a logarithmic factor. This theoretical result was put to the test in Figure 6.8.

Figures 6.8a and 6.8b show that the results holds approximately true in the case of perfectly smooth functions. For nonsmooth solutions (6.8c and 6.8d), the convergence rate of the SDOM is much worse, however, and Figure 6.10 shows that this method produces strong nonphysical artifacts.

To the best of our knowledge, the only weakness in the derivation of the convergence estimate for the SDOM was that we assumed the error functions $\delta u_j$ to be $C^2$ in angle (remember the discussion in Section 5.4). Thus, it seems reasonable to explain our observations with deficient smoothness of the error functions in this case.

## 6.5 Source Iterations

Figure 6.11 shows the solutions of the complete RTE and the convergence of the source iterations for two different values of $\sigma$. We observe exponential convergence in both cases, but the rate of convergence deteriorates with increasing $\sigma$. Since the source iterations are a fixed-point iteration and $\sigma$ is proportional to the change in the right hand sides between consecutive source iteration steps, both findings were to be expected.

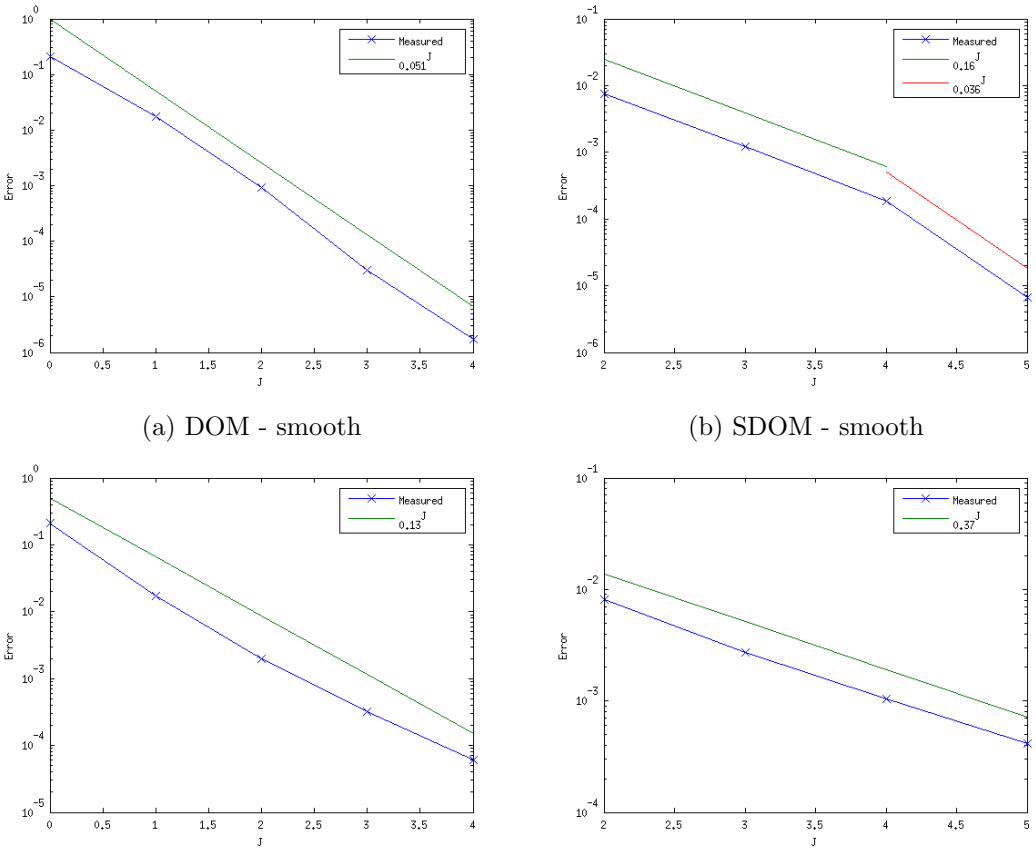


(a) DOM - smooth

(b) SDOM - smooth

(c) DOM - nonsmooth

(d) SDOM - nonsmooth

Figure 6.8: Convergence of DOM and SDOM. In all plots, $\kappa = 4$. In (a) and (b), the source term was

$$f(x, y, \varphi) = e^{-300\left((x-0.5)^2+(y-0.5)^2\right)} e^{-2\min\{\varphi, 2\pi-\varphi\}}$$

whereas in (c) and (d)

$$f(x, y, \varphi) = \max\{0, 1 - 6\ (|x - 0.5| + |y - 0.5|)\}\, e^{-2\min\{\varphi, 2\pi-\varphi\}}$$

$N_s = 4^J$ for the DOM and $b = 4$ for the SDOM was used. The error was measured as $\|G[u](x, y) - G[\tilde{u}](x, y)\|_\Omega$ where $\tilde{u}$ denotes the solution obtained with the indicated parameters and $u$ the reference solution obtained by the DOM with $J = 5$.
CG iterations were aborted once either the relative residual (measured in ridgelet coefficient space) dropped below $10^{-8}$ or 100 iteration steps were executed.

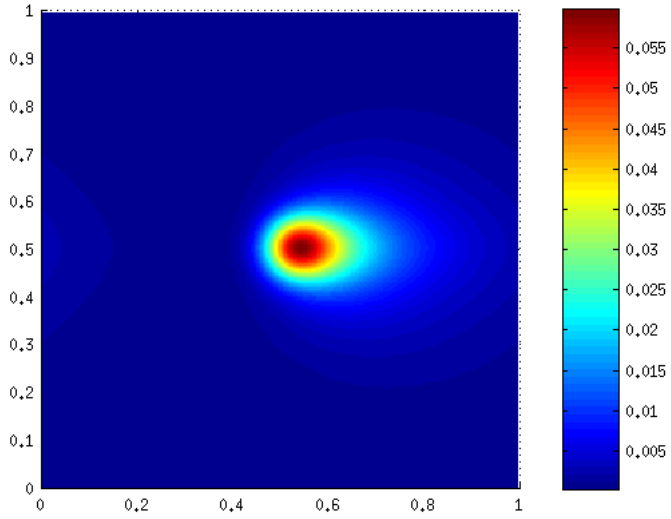


(a) DOM

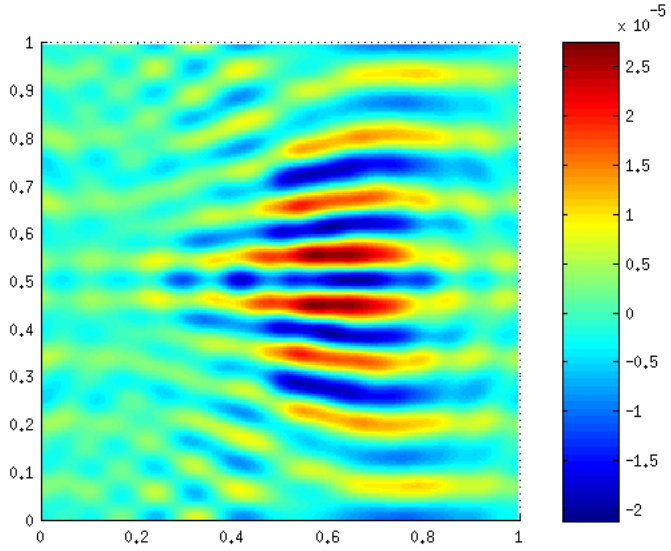


(b) DOM - SDOM

Figure 6.9: Plot of the incident radiation $G[u]$ for $\kappa = 4$ and

$$f(x, y, \varphi) = e^{-300\left((x-0.5)^2+(y-0.5)^2\right)}\, e^{-2\min\{\varphi, 2\pi-\varphi\}}$$

(a) shows the incident radiation obtained with the DOM using $J = 5$ and $N_s = 4^5$. (b) shows the difference between the DOM solution showed in (a) and the SDOM solution obtained with $J = 5$ and $b = 4$.
CG iterations were aborted once either the relative residual (measured in ridgelet coefficient space) dropped below $10^{-8}$ or 100 iteration steps were executed.

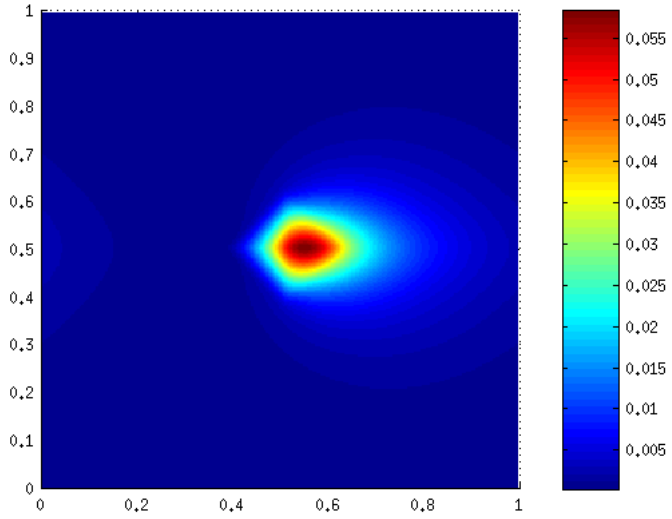


(a) DOM

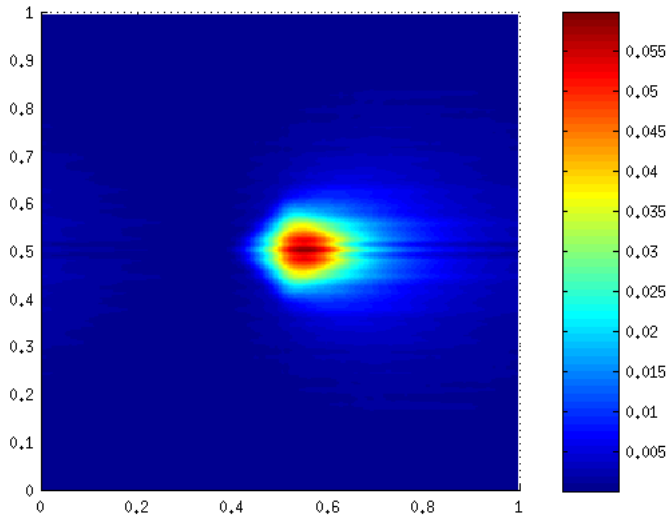


(b) SDOM

Figure 6.10: Plot of the incident radiation $G[u]$ for $\kappa = 4$ and

$$f(x, y, \varphi) = \max\{0, 1 - 6\ (|x - 0.5| + |y - 0.5|)\}\, e^{-2\min\{\varphi, 2\pi - \varphi\}}$$

(a) shows the incident radiation obtained with the DOM using $J = 5$ and $N_s = 4^5$, (b) the SDOM solution with $J = 5$ and $b = 4$.
CG iterations were aborted once either the relative residual (measured in ridgelet coefficient space) dropped below $10^{-8}$ or 100 iteration steps were executed.

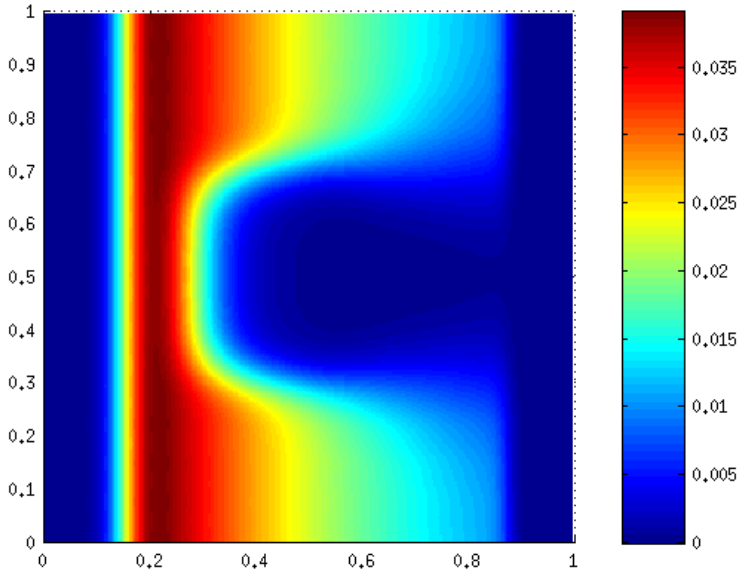


(a) Solution without scattering

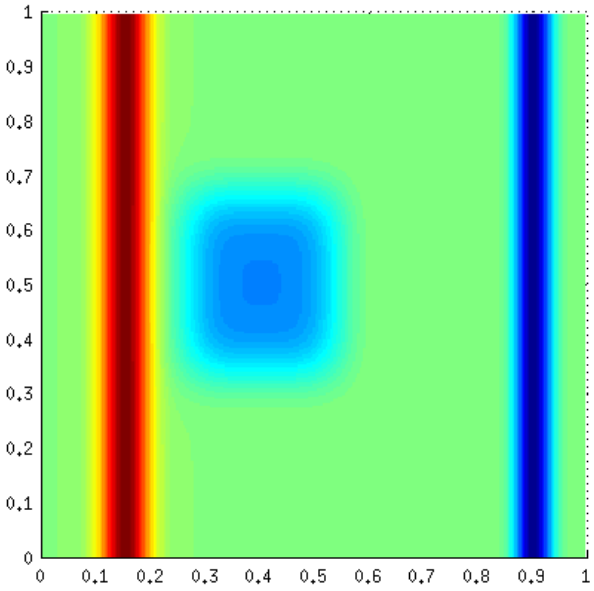


(b) The parameters of the problem.

Figure 6.11: (Continued on next page)

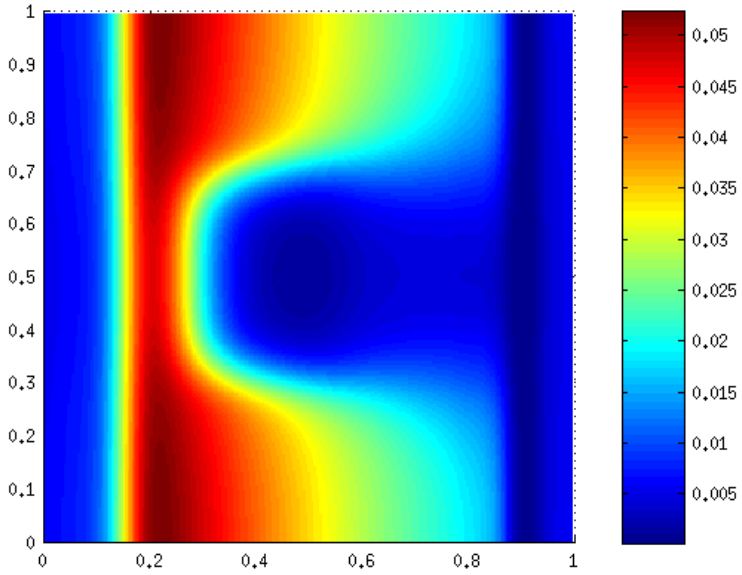


(c) Solution with $\sigma = 0.2$ after 10 source iteration steps

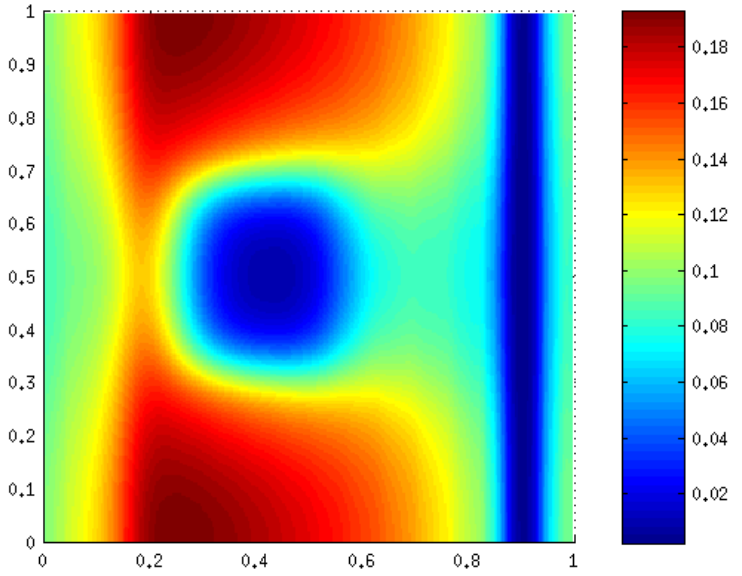


(d) Solution with $\sigma = 0.5$ after 40 source iteration steps

Figure 6.11: (Continued on next page)

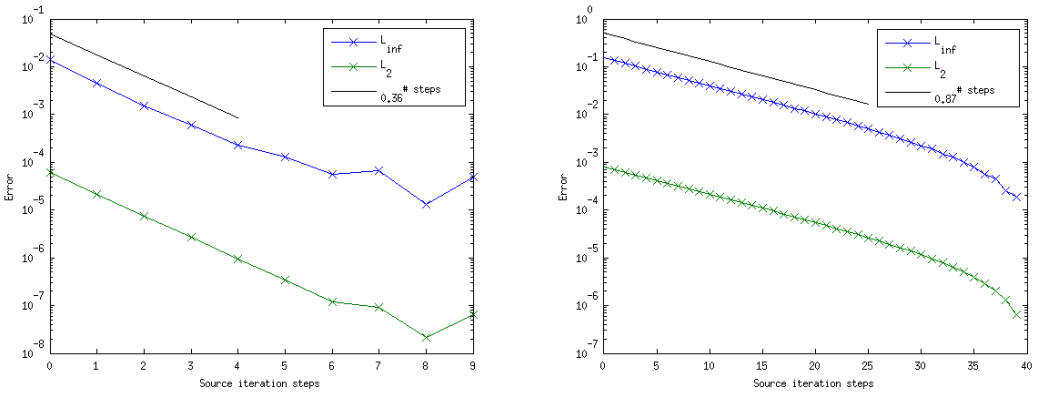


(e) Convergence for $\sigma = 0.2$ (f) Convergence for $\sigma = 0.5$

Figure 6.11: Scattering of radiation around an obstacle. Plots (a), (c) and (d) show the incident radiation for three different value of the scattering coefficient $\sigma$. In (b), the $f$ and $\kappa$ are illustrated: The red line on the left shows the shape of the source term

$$f(x, y, \varphi) = e^{-500\,(x-0.15)^2 - 10\,\min\{\varphi, 2\pi-\varphi\}^2}$$

for some constant $\varphi$. The light blue area in the middle represents the obstacle which corresponds to the second term in

$$\kappa(x, y) = 2 + 18\,e^{-2000\,(x-0.4)^4 - 1000\,(y-0.5)^4} + 98\,e^{-900\,(x-0.9)^2}$$

The last term in $\kappa$, shown in dark blue in (b), was introduced in order to avoid that radiation flows across the $y$-boundary (Compare also with Figure 6.7). Plots (e) and (f) show the convergence of the source iterations for the two nonzero values of $\sigma$. The error was measured as the difference to the solution after 10 (e) or 40 (f) source iteration steps.
We used the SDOM with $J = 5$ and $b = 4$ to solve the RTE for each source iteration step. CG iterations were aborted once either the relative residual (measured in ridgelet coefficient space) dropped below $10^{-4}$ or 100 steps were executed.

# 7 Conclusion

In this bachelor thesis, we devised and studied a ridgelet discretization of the radiative transport equation. For that purpose, we constructed a ridgelet frame and showed that it is large enough to resolve functions without loss of information. We derived and implemented efficient algorithms for the ridgelet transforms, and we showed how they can be used to discretize the RTE at various levels of generality. All of the proposed methods have been successfully tested in numerical experiments, the most important of which was to show that the ridgelet preconditioner proposed and proven theoretically in [1] also works in practice.

This is the first such preconditioner, and its existence raises hope that it is possible to successfully combine the ridgelet discretization with adaptive solvers for linear systems like (5.1), i.e. solvers which only keep track of the most important instead of all coefficients. Such solvers have been proposed already ten years ago, see e.g. [10, 11, 12]). It is a topic of current research by Philipp Grohs and Axel Obermeier to prove the convergence and complexity results from these papers for a ridgelet based adaptive solver for the RTE.

# Bibliography


[1] P. Grohs. *Ridgelet-type Frame Decompositions for Sobolev Spaces related to linear Transport*. Journal of Fourier Analysis and Applications 18/2 (2012), 309-325.

[2] S. Häuser. *Fast Finite Shearlet Transform: a tutorial*. University of Kaiserslautern, 2012

[3] Y. Meyer. *Oscillating Patterns in Image Processing and Nonlinear Evolution Equations*, volume 22. AMS, Providence, 2001

[4] D. Werner. *Funktionalanalysis*, 5. Auflage, Springer-Verlag Berlin Heidelberg 2005

[5] G. Easley, D. Labate, W. Lim. *Sparse directional image representations using the discrete shearlet transform*. Applied and Computational Harmonic Analysis, 25(1), pp. 25-46 (2008)

[6] A. Quarteroni, R. Sacco, F. Saleri, *Numerical mathematics*, vol. 37 of Texts in Applied Mathematics, Springer, New York, 2000.

[7] J. Waldvogel. *Towards a General Error Theory of the Trapezoidal Rule*. Approximation and Computation, Springer, 2011

[8] K. Grella, Ch. Schwab. *Sparse Discrete Ordinates Method in Radiative Transfer*. Computational Methods in Applied Mathematics, pages 305-326, 2011

[9] O. Axelson, G. Lindskog. *On the rate of convergence of the preconditioned conjugate gradient method*. Numerische Mathematik, volume 48, pages 499-523, 1986

[10] R. Stevenson. *Adaptive solution of operator equations using wavelet frames*. SIAM J. Numer. Anal., 41(3):1074–1100, 2003. MR2005196 (2004e:42062)

[11] A.Cohen, W. Dahmen, R. DeVore. *Adaptive wavelet methods for elliptic operator equations - convergence rates*. Math. Comp. 70 (2001), 27-75

[12] A. Barinka, T. Barsch, P. Charton, A. Cohen, S. Dahlke, W. Dahmen, K. Urban. *Adaptive wavelet schemes for elliptic problems - implementation and numerical experiments*. IGPM Report # 173, RWTH Aachen, June 1999